A Review of Recent Advances in the Understanding of Thermomechanical Fatigue Durability and Failure Mechanisms in Nickel-Based Superalloys

J. MOVERARE, R.J. LANCASTER, J. JONES, S. STEKOVIC, and M.T. WHITTAKER

Nickel-based superalloys operate primarily in high-temperature environments where their unique microstructure provides operational capability far in excess of many other engineering materials. As such these materials often operate in applications where thermal cycles occur alongside mechanical fatigue, giving rise to the phenomenon of thermo-mechanical fatigue (TMF). The field of study of TMF has historically been limited due to the need for improved experimental methods to replicate in-service cycles appropriately and provide usable data for component lifing. With the development of international test standards the field has developed rapidly over the past two decades and this paper seeks to review the recent work in the field in the areas of both single crystal and polycrystalline materials to provide a state of the art summary of the current position of the field related to durability and failure mechanisms.

https://doi.org/10.1007/s11661-025-07698-4

I. INTRODUCTION

THERMO-MECHANICAL fatigue (TMF) occurs when a material experiences both cyclic mechanical and thermal loads leading to fatigue and material degradation. In this process, different regions of the material in a component expand or contract at varying rates due to temperature changes, leading to development of uneven thermal strains and internal stresses. These thermal stresses then combine with mechanical loads leading to increased strain accumulation and faster crack initiation. Over time, the combination of thermal and mechanical cycling causes microstructural changes, such as dislocation movement and phase transformations, which further weaken the material. Additionally, time-dependent effects like creep and stress relaxation at elevated temperatures contribute to degradation, ultimately leading to crack propagation and failure. This phenomenon has long been recognised as a critical damage mechanism at elevated temperatures and as such a significant amount of research has been undertaken on ''high temperature'' alloys for a range of applications. In particular, due to their outstanding combination of strength at high temperature and corrosion resistance, nickel-based superalloys are widely employed in challenging environments, most notably gas turbines. These alloys represent an interesting field of study for TMF due to their unique microstructures, with a wide range of studies now available that include both single crystal and polycrystalline alloys. Moreover, in recent years the field has continued to develop rapidly due to the generation of the European code of practice (CoP) for TMF which progressed to the international standards ISO12111[1] and ASTM2368.[2] Further, a new standard for force-controlled TMF testing, ISO 23296:2022, was published in January 2022.[3] These standards, along with further optimisation of temperature measurement techniques, have led to increased consistency of data and the opportunity for greater interpretation.

Historically, the most active area for TMF research was primarily aligned with turbine blade alloys since the proximity to the hot gas stream combined with low mass gives rise to significant thermal transients. These transients, together with mechanical constraints and variation in stresses and temperature over time, will ultimately lead to TMF damage. Over the past 40 years, single crystal alloys have naturally become the preferred material for the first and second stage turbine blade applications, where temperature capability is a stronger performance driver than strength because the turbine efficiency increases with operating temperature. Single crystal alloys outperform polycrystalline materials in this regard because they lack grain boundaries, which are weak points in

J. MOVERARE and S. STEKOVIC are with the Division of Engineering Materials, Department of Management and Engineering, Linköping University, 58183 Linköping, Sweden. Contact e-mail: johan.moverare@liu.se R.J. LANCASTER, J. JONES, and M.T. WHITTAKER are with the Institute of Structural Materials, Swansea University, Bay Campus, Swansea, SA1 8EN, UK.
Manuscript submitted October 14, 2024; accepted January 6, 2025.
Article published online February 12, 2025

polycrystalline materials that can lead to crack initiation and failure under high-temperature conditions. However, as blade temperatures have continued to increase over time, temperatures have increased to a point where TMF effects are now becoming evident in a range of alloys traditionally used for disc applications. Whilst there is no fixed temperature that can be defined where TMF effects require assessment, it is usually deemed necessary to consider the effects in materials that are operating in conditions where high-temperature damage mechanisms such as creep and oxidation become significant. As such, the current paper considers both TMF behaviour in single crystal superalloys, which shows evidence of being a more developed field with extensive data particularly available on the second generation single crystal alloy, CMSX-4, but also in polycrystalline alloys. These polycrystalline alloys can be divided into blade alloys, where temperatures have not required single crystal application, or disc alloys, where increased overall operating temperatures imply that disc alloys require TMF evaluation for in-service component lifing. Since disc alloys are often lifed on the basis of damage tolerant approaches, this has subsequently led to the requirement for greater consideration of crack propagation behaviour under TMF loading.

The current study looks to expand upon previous reviews in this field[4,5] and document the research that has been reported over the past decade on the TMF behaviour of nickel-based alloys. This paper will provide a general overview of TMF behaviour and the subsequent failure mechanisms in nickel-based alloys, recognising that a more mechanistic understanding has been developed for single crystal behaviour, whereas the evolving field of TMF behaviour of disc alloys has led to more of a focus on component lifing. Therefore, this paper covers studies on both TMF crack initiation and crack propagation mechanisms.

Firstly, the paper focuses on single crystal superalloys as their behaviour and damage mechanisms under TMF conditions have been the subject of extensive research. Studies have shown that the TMF life of these materials is influenced by various factors such as the crystallographic orientation of the material, the presence of an oxide layer on the surface, and the phase angle of the thermal and mechanical strain cycles.

Then the discussion will proceed by considering polycrystalline alloys for both blade and disc applications as well as combustor casings. The TMF behaviour of these alloys is more complex due to the interaction of grains with different orientations, which can lead to localised stress concentrations and initiate cracks. The research in this area has increasingly focused on component lifing based on TMF data and understanding of the crack initiation mechanisms, such as the role of persistent slip bands and grain boundaries, as well as the crack propagation phase, which is influenced by factors including the microstructural stability and environmental conditions.

II. THERMO-MECHANICAL FATIGUE (TMF) IN SINGLE CRYSTAL (SX) NICKEL-BASED SUPERALLOYS

Nickel-base single crystal superalloys (SX-alloys) are mainly used for turbine blades in aero-engines and high-performance industrial gas turbines for power generation. Such parts are critical components that often limit the durability and performance of gas turbines. Therefore SX-alloys are designed to withstand extreme conditions of temperature and loading during operation.[6] In addition, the introduction of thermal barrier coatings and sophisticated cooling systems typically lead to complex thermal and mechanical loadings, especially during engine start-up and shut-down operations that makes SX-alloys components prone to TMF failure.[7]

SX-alloys are typically cast with the $\langle 001 \rangle$ direction along the axial direction of the turbine blade, but also often with a controlled secondary orientation to reduce stresses in critical regions. The typical microstructure consists of cuboidal γ' precipitates orientated along the $\langle 001 \rangle$ direction in a matrix of γ and the most commonly used alloys belong to the second generation of SX-alloys with 3 wt pct of rhenium and up to 65 vol pct of γ'.[8] Since γ and γ' are coherent and both have an FCC crystal structure, the SX-alloys display very anisotropic mechanical properties. As an example, the elastic properties of SX-alloys are rather similar to that of pure Ni in single crystal form, which is $E_{\langle 001 \rangle} = 125$ GPa, $E_{\langle 011 \rangle} = 220$ GPa and $E_{\langle 111 \rangle} = 294$ GPa at room temperature. Other properties such as tensile and creep are also highly anisotropic, but the mutual order between the directions also depends on temperature and chemistry. The anisotropic properties have a strong impact on the deformation and damage behaviour of SX-alloys during TMF.

Damage mechanisms in TMF include fatigue damage, creep damage, oxidation damage and microstructural transformations[8,9] and their impact and synergy depend on the corresponding temperature and load cycle. For SX-alloys the degradation of the microstructure, typically coarsening or rafting of the γ' precipitates as well as a tendency for recrystallisation and formation of TCP-phases, also plays an important role in the damage development.[7]

For an in-phase (IP) TMF cycle, the tensile loading coincides with the high-temperature part, reaching the maximum temperature (T_{Max}) of the cycle and deformation is characterised by high-temperature creep in tension and low temperature plasticity in compression. For a turbine blade this situation may occur, for instance, near cooling holes or at structures inside cooling channels. However, the stresses/strains from thermal gradients can also be superimposed by external loads such as internal pressure and centrifugal forces which will further increase the tensile stress at elevated temperature.[10] The combination of tensile stresses at an elevated temperature and significant hold times will promote creep, which may have a considerably detrimental effect on TMF performance even for rather moderate temperatures.

The situation during an out-of-phase (OP) TMF-cycle is completely different, where the material undergoes creep relaxation in compression at high temperatures and plastic deformation in tension at low temperatures. This is the situation found at "hot-spot areas", *i.e.*, small regions with higher temperature than the surrounding material. This may occur on, for example, a turbine blade aerofoil or platform due to insufficient cooling. Since these areas will be in compression during the high-temperature running period of the engine or turbine, high-temperature creep relaxation will cause the material to be in tension at shut-down. Furthermore, the oxides formed at elevated temperature have been identified as an important factor for the TMF life of SX-alloys since their low ductility promotes cracking in tension often resulting in lower OP lives than IP. Figure 1 illustrates a series of OP–TMF tests conducted on 1st and 2nd generation Ni-based SX-alloys. The graph clearly indicate that the TMF life decreases with increasing maximum temperature and strain amplitude, while the data are fairly consistent between the different alloys.

Since SX-alloys are highly anisotropic and do not contain any grain boundaries, the deformation is often highly localised, which adds an extra complexity when interpretating the results generated on these materials. In addition, deformation twinning is frequently observed and crack growth predominantly occurs along the twins in a very localised manner until failure, typically accompanied by recrystallisation.[7] When deformation primarily occurs along deformation bands that extend across the complete cross section of the specimen, as seen in Figure 2, the interpretation of the results can be difficult if there is a gradient in stress and temperature along the deformation band. In addition, this non-uniformity can lead to variations in the material's response to the applied stress, making it difficult to predict the material's behaviour accurately. The development of these deformation bands is therefore crucial for the TMF damage of SX-alloys and has been found to depend on crystal orientation, phase angle and dwell time.

Due to the development of the localised deformation bands, fatigue crack paths in SX-alloys deviate from the conventional Stage I/Stage II pattern. Instead, it is common for cracks to initiate with Mode I opening and later shift towards crystallographic shearing. Various factors, such as temperature, strain range, dwell periods, microstructure, crystal orientation, environment, strain–temperature phasing in TMF, and frequency, collectively influence the crack paths observed.[12] In OP–TMF, the high temperatures align with compressive stresses, activating mechanisms such as oxidation–fatigue interaction and γ' coarsening, especially above 800 °C, which intensifies crack growth due to oxidation. In IP–TMF, cracks form at weak interfaces, while OP–TMF cracks form at oxide spike sites. Bithermal OP–TMF cycles, with mechanical loading at temperature extremes, further promotes oxidation-assisted crack growth, resulting in sharp, planar cracks.[12]

A. *Influence of Crystal Orientation*

In a strain-controlled TMF test of an SX-alloy, the elastic stiffness of the material with respect to the loading direction is the strongest factor in determining the TMF life for a given mechanical strain range. This is illustrated in Figure 3 from the work of Segersäll *et al.*[11,13] where the [001] oriented specimens with a lower stiffness exhibit longer fatigue life. The main explanation is that for a given mechanical strain range a lower stiffness will render lower stress ranges which is

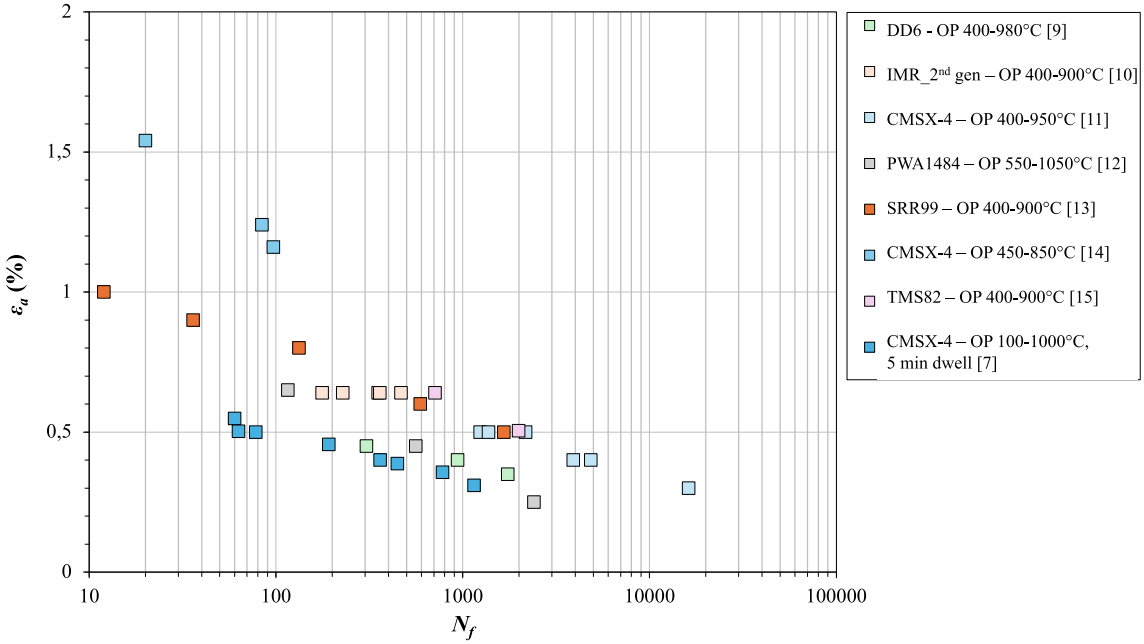

Fig. 1—OP–TMF results for a range of different 1st and 2nd generation Ni-based SX-alloys. Reproduced using data from Refs. [7,9–15].

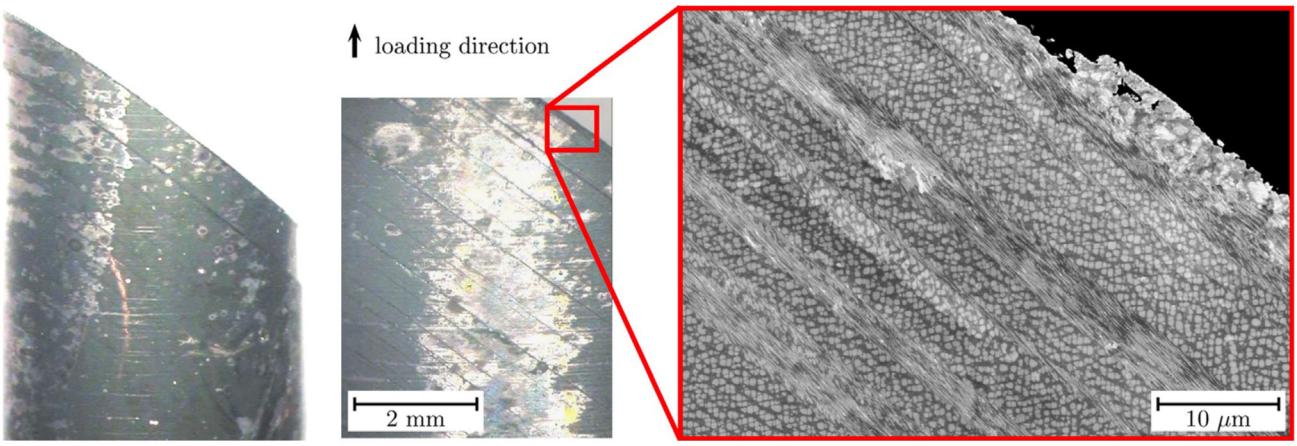

Fig. 2—Typical appearance of deformation bands in an SX-alloy during TMF (Reprinted with permission from Ref. [11]).

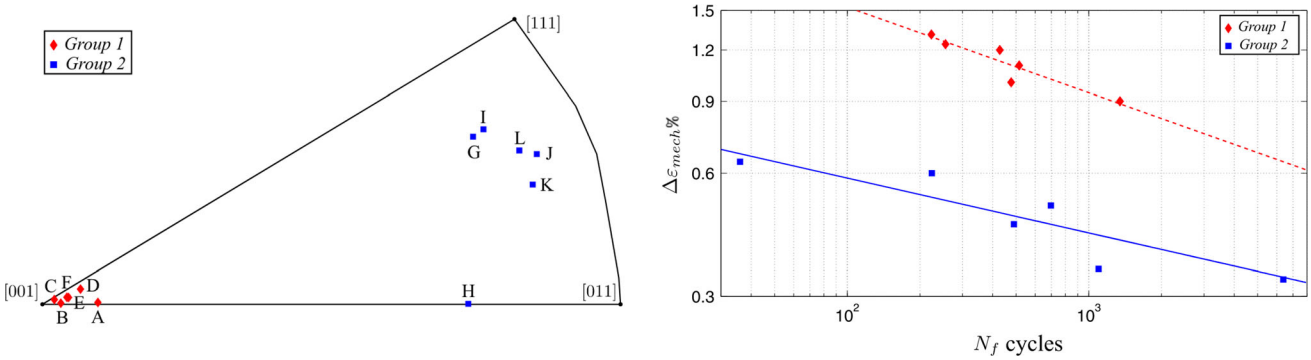

Fig. 3—OP–TMF testing of an SX-alloy in different crystallographic orientations. (*a*) The orientations of the investigated test specimens in the stereographic triangle. (*b*) Mechanical strain range *vs* number of cycles to failure (Reprinted with permission from Ref. [11]).

beneficial for fatigue. In addition, the number of active slip systems during deformation was also found to influence the OP–TMF life. A higher number of active slip planes seems to be beneficial since the deformation in this case becomes more widespread and less localised.

Similar results were found by Luo *et al.*[14] who studied the anisotropic TMF behaviour under both IP and OP loading conditions and found that the fatigue lives under the same mechanical strain range obeyed $\langle 001\rangle > \langle 011\rangle > \langle 111\rangle$ in most cases. The $\langle 001\rangle$ specimens primarily underwent elastic cycling, whereas the $\langle 011\rangle$ and $\langle 111\rangle$ specimens displayed plastic deformation at higher strain levels. Analysis of the resulting fracture surfaces revealed creep facets due to creep damage, which were governed by octahedral slip systems in $\langle 001\rangle$ and $\langle 011\rangle$ specimens, while cubic slip systems predominated in the $\langle 111\rangle$ specimens. Pronounced rafting of the γ/γ' microstructure was only found for testing of $\langle 001\rangle$ specimens. In addition, it was found that the TMF lives were reduced by 70 to 90 pct when compared with isothermal fatigue conducted at the peak temperature of the TMF test. OP–TMF was also found to be more detrimental than IP-TMF for all crystallographic orientations and strain ranges due to the increased extent of cyclic hardening and the resulting higher mean stress observed under this loading regime.

Due to the elastic anisotropy, it is often preferred to use a stress-based approach to evaluate TMF life of SX-alloys. In the study by Smith *et al.*[15] an extensive set of TMF and isothermal fatigue data for CMSX-4 was analysed and it was found that the influence of crystal orientation, load cycle and temperature were well captured by a lifing model based on the Walker corrected stress. Also in the work by Amaro *et al.*[16] where a more mechanism-based life model was derived, it was found that kinetics of the microstructure degradation as well as the relative amount of damage contributed to by the inelastic strain were found to be dependent upon the applied stress.

B. *Influence of Phase Angle (OP vs IP)*

Han *et al.*[17] investigated the TMF fatigue behaviour of an $\langle 001\rangle$ oriented SX-alloy under different cycles of strain and temperature. It was found that the fatigue lives under IP-TMF were longer than those of OP–TMF, and the maximum tensile stress level was concluded to be the lifetime-limiting factor. Compared to the low-cycle fatigue (LCF) lives achieved under isothermal conditions at the corresponding T_{Max} of 900 °C, the lifetime during TMF was significantly reduced. From analysis of the fracture surfaces and

microstructural changes, creep emerged as the primary damage mechanism during IP-TMF, whereas oxidation contributes to shorter life in OP–TMF tests.

Also Hong *et al.*[18] found that despite a smaller inelastic strain range and lower mean stress level during OP–TMF 400 °C to 950 °C compared to LCF at 950 °C, the OP–TMF life was less than half of the LCF life. Notably, during OP–TMF cycling, the maximum tensile load at the minimum temperature (T_{Min}) accelerated surface crack initiation and propagation. During OP–TMF cycling, clusters of parallel twin plates emerged on the {1 1 1} planes ahead of the crack tip upon reaching a specific size. The localized twins served as a preferential path for crack propagation. During LCF, deformation seems to rely more heavily on diffusion mechanisms, whereas in OP–TMF, partial dislocation movement with the $\{1\ 1\ 1\}\langle 112\rangle$ slip system appears to dominate, leading to the creation and advancement of deformation twins.

Kersey *et al.*[19] studied OP–TMF crack growth from laser drilled holes in an SX-alloy and found that the majority of crack propagation took place at the low temperature portion of the TMF-cycle. However, crack propagation under TMF loading conditions with a T_{Max} of 1038 °C or 1149 °C is considerably faster than the corresponding isothermal LCF crack growth at $T = T_{Max}$ and similar loading conditions as for the tensile part of the TMF cycle. This indicates that there is noticeable damage accumulation during the high-temperature compressive load portion of the cycle. Similar results were found by Palmert *et al.*[20] where the microstructural investigations suggests that local dissolution of γ' and recrystallisation at the crack tip is the most likely explanation for the observed difference in crack growth rate between LCF tests at 100 °C and OP–TMF tests with a minimum temperature of 100 °C. However, interestingly this work also concluded that by taking the crack closure effect into account for OP–TMF tests, the crack growth rates *vs* ΔK_{eff} collapse along one trendline within a factor 3 scatterband independent of T_{Max} and length of the dwell time.

Palmert *et al.*[20] also investigated crack growth behaviour during force-controlled experiments and found that during IP–TMF, unlike OP–TMF, there was no notable distinction in the crack growth rate *vs* ΔK_{eff} compared to isothermal tests at the corresponding T_{Max}. Furthermore, it was found that even if the crack growth rate increased when a hold time was applied at T_{Max}, this increase in crack growth rate is due to a reduction in crack closure, resulting in an increase in the effective stress intensity factor range which accelerates the cycle-dependent crack growth. Therefore it was possible to describe all IP–TMF and LCF tests up to a maximum temperature of 850 °C regardless of dwell time, by one trend line when plotted as crack growth rate *vs* ΔK_{eff}.

Yang *et al.*[21] and Ai *et al.*[22] performed stress controlled TMF testing in the temperature range 500 °C to 980 °C and found that under identical temperatures and mechanical loading conditions, IP-TMF exhibits the shortest fatigue life, with LCF falling between the IP and OP conditions. Moreover, the trend of lifespan variation with phase angle under stress control differs notably from that under strain control, since the OP TMF lifetime was considerably longer than the IP-TMF lifetime at identical stress levels. Additionally, as it will be discussed in the next section, introducing a high-temperature dwell time significantly reduces IP-TMF lifetime, which is notably shorter (measured as time to failure) than that of creep under T_{Max} and maximum stress (σ_{Max}), primarily due to the ratcheting effect.

C. *Influence of Dwell Time*

During OP–TMF testing of SX-alloys, highly localised twinning has been found to be one of the main deformation mechanisms.[7,23–25] Zhang *et al.*[26] found that for OP–TMF cycling without a compressive hold time, the crack initiates at the surface and initially grows perpendicular to the stress axis followed by propagation along a twin plate. For TMF cycling with a compressive hold time (ranging from 10 mins to 10 hours), the main crack propagates directly along the inclined twin plate until final failure. Furthermore, even if the dwell time occurs in compression, the number of cycles to failure rapidly decreased, as the dwell time increased as seen in Figure 4. This is believed to be a combined effect from the change in deformation mode and the stress relaxation during dwell which increases the amount of inelastic strain in each cycle, but also leads to the development of a tensile mean stress (σ_{Mean}). For IP–TMF, models combining fatigue damage and creep damage have been successfully applied to rationalise the effect of dwell time both for crack initiation[27] and crack propagation.[28]

The introduction of dwell times in TMF is important to study since they are often necessary to accurately simulate component-near operating conditions, especially for single crystal turbine blade applications. However, other component-near features might also be important to envisage in testing such as thermal

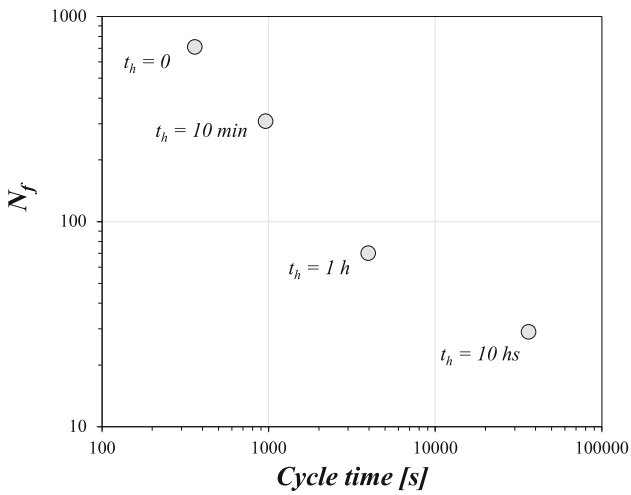

Fig. 4—Influence of dwell time (t_h) on the number of cycles to failure during OP–TMF (400 °C to 900 °C) of the SX-alloy TMS-82. All tests with a mechanical strain range of 1.28 pct. Reproduced from data presented in Ref. [26].

gradients. Modern high pressure SX turbine blades have internal cooling and are externally thermally protected using a thermal barrier coating (TBC) system. These material systems are submitted to very complex service conditions, with a combination of mechanical and thermal fatigue under complex thermal gradients. Experimental studies to address this typically involve thermal-gradient-mechanical fatigue (TGMF) testing.[29]

D. *Microstructural Aspects of TMF*

1. *Influence of rafting and minimum temperature (T_{Min})*

The phenomenon of yield strength anomaly in the pure γ'-phase is well-documented,[30] yet its implications on TMF of γ–γ' alloys and the influence of T_{Min} are often overlooked.[31,32] Both the γ matrix and the γ' precipitate exhibit relatively low strength at room temperature and the notably high initial yield strength of SX-alloys results from a favourable interaction between the matrix and precipitate in the carefully optimised, albeit thermodynamically unstable, initial cuboidal microstructure. Consequently, any deviation from this optimised microstructure naturally leads to a reduction in yield strength,[33] especially at low temperatures. Since rafting occurs during TMF tests involving high T_{Max} and dwell times, the material eventually will yield at a lower stress level compared to its virgin condition, especially at the cold end of the TMF cycle. This effect will be amplified by decreasing values of T_{Min} in the TMF-cycle. As the material yields at a reduced stress level, it results in a higher inelastic strain range and consequently in a reduced crack initiation life. This effect was illustrated for CMSX-4 in the work by Arrell *et al.*[31], where TMF life decreased by a factor of 3 when T_{Min} was reduced from 400 °C to 100 °C. Similar behaviour has also been reported for directionally solidified superalloys.[32]

Kirka *et al.*[34] also studied the effect of different aged microstructures on TMF behaviour under either continuously cycled (CC) with a triangular waveform or creep-fatigue (CF) with a dwell time at T_{Max}. A wide range of temperature ranges and dwell times were investigated with T_{Min} of 100 °C or 500 °C and T_{Max} of 750 °C, 850 °C or 950 °C. Three different aged microstructures, generated through accelerated aging and pre-creep treatments, were studied: stress-free coarsened γ', rafted with orientation perpendicular to loading direction (N-raft), and rafted with orientation parallel to loading direction (P-raft). For the CF test conditions, a 1200 second strain hold was applied at the peak temperature. In general, the aged microstructures showed lower resistance to TMF compared to the virgin microstructure, but not for all cases. The effect of an aged microstructure on life is summarised in Table I. Lou *et al.*[14] studied the rafting formed during TMF cycling and found that during testing of ⟨001⟩ oriented specimens, the rafting of the γ/γ' microstructure was of N-type for IP-TMF and of P-type for OP–TMF.

2. *Slip and twinning*

As already mentioned in previous sections, highly localised twinning has been found to be the main deformation mechanism during TMF, especially of 2nd generation (Re containing) SX-alloys. The formation of these twins has been extensively studied for ⟨001⟩ oriented SX-alloy under OP loading, see *e.g.*, References 7, 24, and 35 through 39 During OP–TMF testing of specimens oriented along the ⟨001⟩ direction, twinning will occur during compression at elevated temperature. Experimental results by Kolbe[40] have confirmed that microtwinning above 700 °C requires the passage of $a/6\langle 112\rangle$ partial dislocations through both γ' and γ phases, as well as a diffusion-mediated reordering in the wake.

In the study by Segersäll *et al.*,[41] OP–TMF testing was performed on ⟨011⟩ oriented samples and for this direction twinning was less frequently observed; especially at high strain ranges. Instead, deformation occurred in very localised deformation bands by slip and cutting of the γ' particles along the {111} planes. The orientation of the single crystal relative to the applied load is thus important for the formation of deformation twins during TMF. In addition, different

Table I. Summary of the Effect of Aged Microstructure on Life Compared to Virgin Microstructure

Microstructure	TMF Condition	Life Effect	Reason
Stress-Free Coarsened	CC IP	↓	aged maintains higher tensile mean stress due to the absence of internal stresses that can relax
Stress-Free Coarsened	CF IP	—	dwell provides sufficient time to age virgin microstructure and equalise hysteresis responses
N-Raft	CC IP	↓	aged maintains higher tensile mean stress due to the absence of internal stresses that can relax; raft orientation facilitates fatigue crack propagation
N-Raft	CF IP	—	dwell provides sufficient time to age virgin microstructure and equalise hysteresis responses
P-Raft	CC OP	↓	reduced cyclic strength resulting in greater accumulated cyclic inelastic strain due to shearing of γ' at lower temperature part of cycle
P-raft	CF OP	↑	inability to shear γ' rafts during high-temperature dwell resulting in beneficial crack deflection promoted by oxygen penetration along the γ/γ' interfaces

Reproduced with permission from Ref. [34].

deformation behaviour can be expected for IP and OP–TMF, where the ⟨001⟩ direction usually exhibited more pronounced twinning during OP–TMF deformation, while the ⟨011⟩ direction showed more pronounced twinning during IP-TMF.[13] The observed influence of orientation and phase angle on the twin formation is consistent with the model of Kolbe[40] where microtwining is expected under compressive stress for ⟨001⟩ oriented crystals and under tensile stress for ⟨110⟩ oriented ones.

It also appears as if twinning is less pronounced in Re-free 1st generation SX-alloys.[42,43] For these SX-alloys slip typically occurs along the {111} planes without the presence of twins but still in a highly localised manner. This clearly indicates that composition has an effect on deformation behaviour during TMF. However, only very few studies have been conducted to explore the influence of composition on TMF life. In the study by Segersäll *et al.*,[44] the impacts of alloying with either Si or Re were examined. The study focused on OP–TMF, with additional static creep deformation tests to provide further insights into the observed effects. A notable Si-effect was discovered where a modest addition of 0.25 wt pct Si doubled the TMF life. This enhancement was attributed to a higher yield stress at T_{Min} and narrower slip bands which increased the resistance to recrystallisation and cracking. On the other hand, alloying with Re, while significantly improving creep behaviour compared to Si, does not exert as strong an influence on TMF life as TMF life is usually influenced by more than just creep.

A compositional effect on TMF has recently also been reported by Ge *et al.*[45] The effect of Ru addition on the deformation mechanism of an SX-superalloy with Re under OP–TMF in the temperature range 400 °C to 900 °C was investigated and it was found that there was a significant increase in OP–TMF life by the addition of 3 wt pct Ru. The introduction of Ru results in the formation of numerous stacking faults with varied orientations within the γ matrix. This phenomenon is associated with the increased strength of the alloy matrix and a decrease in stacking fault energy. Conversely, in the absence of Ru, the alloy matrix exhibits weaker characteristics, leading to the generation of numerous dislocations within the γ matrix. Additionally, more twins are formed, extending across both the γ and γ' phases. As a result of the generation of stacking faults and potentially fewer twin dislocations within the γ matrix, the occurrence of twins was observed to be restrained in the Ru-doped alloy in contrast to the Ru-free alloy. This suppression of twins is likely a significant contributing factor to the extended life under OP–TMF.

III. THERMO-MECHANICAL FATIGUE (TMF) IN POLYCRYSTALLINE (PX) NICKEL-BASED SUPERALLOYS

This section attempts to provide an overview of the published work in the area of polycrystalline nickel-based superalloys, recognising that the typical in-service temperature of the alloys considered will vary, usually as a function of their chemistry. Therefore, alloys are considered, broadly speaking, in terms of application, and are considered as below:

(i) Alloys used for disc applications,
(ii) Alloys used for blade applications where single crystal materials were not required and polycrystalline materials have been employed,
(iii) Alloys used in other applications such as combustor casings.

A. *Forged Alloys for Disc Applications*

Forged nickel-based superalloys are commonly used for disc applications due to their superior mechanical and metallurgical properties. The forging process, which involves the use of compressive forces to deform heated metal into the desired shape, results in predictable and consistent grain sizes leading to several benefits such as better part quality and greater strength. In the context of disc applications, a specific example is the development of powder metallurgy superalloys with a microstructure typically consisting of fine, uniformly distributed gamma-prime (γ') precipitates within a gamma (γ) matrix. This microstructure gives better creep resistance and tensile strength at high temperatures making them ideal for demanding high stress environments. These alloys can be engineered with a specific composition and microstructure tailored to meet the stringent requirements of critical components such as turbine discs and blades. TMF resistance is particularly critical in these applications, as it ensures the alloys can maintain their integrity under such loadings.

The following section provides an overview of several key forged Ni-based superalloys, including Inconel 718, Waspaloy, and RR1000 as each of these alloys have attracted significant research efforts in the area of TMF in recent years.

1. *IN718*

Inconel 718 (IN718) is an age-hardened alloy that has mainly found use in applications with high strength requirements in the gas turbine sector and has particularly found application as a disc alloy, providing an appropriate balance of properties at a reasonable cost, when temperatures exceed the capabilities of traditional Ti-based alloys. This alloy is often considered slightly different to conventional nickel-based alloys due to the inclusion of Nb, which forms a secondary precipitate, γ'', which is primarily responsible for hardening in the alloy. Since this precipitate is metastable, transforming to δ following exposure at higher temperatures, in-service operation of the alloy is limited to approximately 650 °C.

Over the past decade, IN718 has been one of the most researched Ni-based polycrystalline superalloys in terms of TMF behaviour. Sun *et al.*[46,47] undertook two studies on the alloy, firstly in 2019[46] to investigate the uniaxial and multi-axial TMF behaviour of IN718 and in 2020[47] to simulate thermal gradient mechanical

fatigue (TGMF) in the material. The two studies were supported by a series of TMF and TGMF tests to formulate a novel constitutive model to capture the complexities of multi-axial thermo-mechanical cyclic plasticity. The TMF test programme consisted of a series of IP and OP TMF experiments performed on solid and tubular round bar specimens under a temperature range of 300 °C to 650 °C, as compared to tests performed under isothermal conditions at T_{Max} and T_{Min}. The authors found that for all tests conducted across the alternative phase angles with a non-zero mean mechanical strain, the resulting hysteresis stress-strain loops consistently exhibited cyclic softening behaviour before stabilising as the cycle number increased. In the IP test, a reduction in σ_{Mean} was observed, whilst in the OP test, an increase in σ_{Mean} occurred.[46] Within this work the OP tests consistently outperformed the IP experiments, whilst exhibiting a similar fatigue performance to the isothermal tests carried out at T_{Max}.[46,47] For the TGMF tests, the dominant failure mechanism changes with the phase angle of the thermal and mechanical loading. Intergranular fracture plays a dominant role under TGMF-IP while transgranular crack growth is predominant during TGMF-OP tests.

Deng *et al.*[48] performed a similar study on IN718, investigating the IP and OP TMF behaviour under a temperature range of 350 °C to 650 °C and comparing to the material tested under isothermal conditions at both T_{Min} and T_{Max}. Like that observed by Sun *et al.*[46,47] the OP condition was found to be less detrimental to fatigue life than the IP equivalent, whilst also outperforming the isothermal fatigue tests carried out at T_{Max}. As would be expected, the dominant mode of crack propagation under IP and isothermal tests performed at T_{Max} involved intergranular fracture, whereas under OP and isothermal experiments at T_{Min}, the fracture mechanisms are primarily characterised by transgranular crack growth. Under all conditions, the material saw an increase in plastic deformation and cyclically softened with an increase in cycles.

Böcker *et al.*[49] observed a similar behaviour under a higher T_{Min} of 400 °C. They performed several tests on IN718 with a temperature cycle of 400 °C to 630 °C under both IP and OOP loading and considered how the material deforms under planar-biaxial TMF conditions using cruciform specimens. The results showed that IN718 cyclically softened under all loading conditions, whilst σ_{Mean} under IP loading became more compressive with cycling, whereas it developed to a more tensile stress in the OP tests. As seen in the other studies, here, the OP condition generally outperformed the tests undertaken under IP loading and was comparable to isothermal tests performed at T_{Max}, however, results fell considerably short of isothermal tests at T_{Min}. Cracks initiated from non-metallic inclusions at the surface in both cases.

2. *Waspaloy*

Waspaloy represents a more traditional approach to the development of a nickel disc alloy, being an age-hardened alloy that has been used in-service for over 60 years. Through this time significant refinement of the alloy has taken place, resulting in increased tensile strength which has sustained the use of the alloy in the power generation industry. In general, IN718 shows higher strength for lower temperatures (up to 700 °C), but Waspaloy tends to retain strength more effectively at the higher end of its operating temperatures (up to 870 °C depending on specific applications).

Kulawinski *et al.*[50] conducted a comprehensive examination of the isothermal and thermomechanical fatigue (TMF) characteristics of Waspaloy, considering both uniaxial and multiaxial loading conditions on cruciform specimens. They subjected the material to IP and OP TMF tests with a temperature range of 400 °C to 650 °C, where heating was supplied *via* an induction coil. In IP loading, Waspaloy exhibited either cyclic hardening or cyclic softening after an initial stable period, dependent on the applied strain rate, with the transition from softening to hardening occurring with an increase in applied strain range. OP TMF experiments showed a comparable trend, with a continuous decrease in σ_{Mean} for applied strain amplitudes up to 0.6 pct, whereas at 0.8 pct, the material was cyclically stable. The cyclic stability at higher strains was attributed to the tensile σ_{Mean} induced by the maximum tensile stress at T_{Min}, unlike IP tests where the σ_{Mean} remained in compression. Cracks were initiated along slip planes and twin boundaries, with micro cracks forming in grains under the biaxial stress states.

Further work by the same author associated the observed TMF response of Waspaloy under both IP and OP conditions with the movement of dislocations. Referring to Clavel and Pineau's findings,[51,52] they noted that high strain amplitudes lead to a homogeneous dislocation distribution under isothermal conditions, while lower strain amplitudes result in a planar dislocation structure. The authors linked planar slip with the formation of surface intrusion and extrusion step features, serving as initiation points for crack formation and the onset of TMF damage.

Regarding crack propagation, Kulawinski *et al.*[50] highlighted a shift in mechanisms at different temperatures. Under isothermal loading at 400 °C, transgranular crack propagation was prevalent, while at 650 °C, intergranular propagation dominated due to increased oxidation at grain boundaries. A similar shift in crack growth mechanisms was observed in high strain amplitude TMF tests, where intergranular crack growth prevailed in IP tests, contrasting with transgranular propagation under OP loading. However, at low strain amplitudes both IP and OP tests showed intergranular crack growth, presumably as time-dependent mechanisms contributed more to the overall crack growth behaviour. Despite these variations, the authors found that the IP and OP TMF life of Waspaloy could be conservatively estimated by LCF tests at T_{Max}.[50]

3. *RR1000*

RR1000 is a more recently developed nickel disc superalloy utilising similar metallurgical principles as found in Waspaloy, albeit with a higher fraction of γ' forming elements which are then used to form a trimodal distribution of precipitates. Much of the

research on TMF undertaken on RR1000 has been performed at Swansea University[53–58] and through the associated EU funded project, DevTMF.[59,60] Over the past decade, a wide range of TMF tests across different phase angles including IP, OP, clockwise diamond 90 deg (CD90°), counter-clockwise diamond 90 deg (CCD90°), 45 and − 135 deg at temperature ranges of 300 °C to 700 °C and 300 °C to 750 °C were performed. Results have been reported under both strain-controlled fatigue conditions and load controlled crack growth experiments to understand the crack initiation and propagation behaviour of the alloy.

In the paper published in 2017 by Jones *et al.*,[54] the influence of phase angle, strain range and peak cycle temperature were all investigated using tubular specimens and compared to the damage behaviours observed under isothermal conditions. They found that, in general, the TMF tests performed under the various conditions were more damaging on fatigue life compared to the equivalent isothermal experiments undertaken at T_{Min} and T_{Max}. Each of the different phase angles were found to exert a substantial influence on the evolution of the cyclic σ_{Mean}, deformation, and damage behaviour, the extent of which is also controlled by the employed strain range and/or peak cycle temperature used. The T_{Max} temperature (700 °C and 750 °C) was found to be particularly important, influencing the extent of stress relaxation and the subsequent cyclic softening under IP loading, and cyclic hardening under OP conditions. In both instances, the increased evolution of cyclic σ_{Mean} at the higher T_{Max} temperature resulted in a reduction in the TMF lives as compared to the lower T_{Max} of 700 °C.[54]

Throughout the different experiments, the IP conditions were proven to be the most detrimental to TMF life, particularly at strain amplitudes above 0.4 pct, whilst the OP condition was shown to be the least damaging (IP < − 135 deg < 45 deg < CD90 deg < CCD90 deg < OP). In the IP experiments, creep damage at grain boundary locations emerged as the dominant damage mechanism, leading to accelerated intergranular cracking. However, under an applied strain amplitude of less than 0.4 pct, the authors reported a change in the dominant damage mechanism, whereby the OP condition became more detrimental on TMF life than IP experiments. This was attributed to accelerated surface oxide crack initiation at low temperatures becoming more prevalent under OP loading, facilitated by an evolving tensile σ_{Mean} and resulting in a mix of intergranular and transgranular cracking. This behaviour was also most likely influenced by an initiation period of fatigue cracks, with high strain tests initiating fatigue cracks almost immediately so that the dominant influence on fatigue life was the rate of TMF crack propagation. Similar responses were observed in 45 and − 135 deg tests, with the 45 deg experiments experiencing similar behaviours to the IP conditions, whilst the − 135 deg tests behaving more akin to OP conditions. The authors also explored the influence of cycle direction, where the 90 deg diamond cycles were directly compared in both the clockwise and counter-clockwise directions. They found there was no pronounced difference between the two since there was no significant accumulation of σ_{Mean}, resulting in similar lifetimes with no discernible effect of cycle direction.[54]

Gray *et al.*[56] furthered this work by taking a more holistic approach to understanding the contrasting damage mechanisms under the different phase angles. They commented that since maximum strain coincides with T_{Max} under IP conditions, the tensile stress during this loading serves to open the crack, while the elevated temperature promotes oxygen diffusion. Consequently, oxygen preferentially accumulates along the grain boundaries. This leads to the creation of an oxide wedge at the crack tip and the weakening of grain boundaries by the formed oxide. As a result, crack growth is accelerated along these oxide-weakened grain boundaries. In contrast, under OP conditions, the damage behaviour closely resembles that observed under isothermal fatigue, involving crack propagation and transgranular failure. The diminished influence of oxidation in OP TMF crack growth can be explained by its occurrence at the minimum stress. In OP TMF, oxidation predominantly takes place after the crack has closed, thereby preserving the sharpness of the crack tip, and facilitating propagation along the transgranular {111} plane. Since the crack is under compression during the oxidation process, oxygen is unable to diffuse far enough to significantly impact the crack tip.[56]

To further investigate the influence of crack propagation behaviour on the total fatigue life, there have also been several studies focusing on the TMF crack growth (TMFCG) behaviour of RR1000.[53,55,57,58] Although methods have been developed to predict crack growth rates under isothermal conditions over a wide range of temperatures, frequencies and load ratios, only very few published studies on crack growth under TMF conditions on superalloys were available over recent years. Furthermore, since the translation of isothermally obtained fatigue crack growth data into a true TMF context was also questionable, the need for more experimental studies in this field was obvious. The open literature revealed only a limited amount of information regarding TMFCG testing, with isolated publications investigating growth rates under both IP and OP by use of a range of the different methodologies. The first of a series of papers on RR1000 was published in 2017 by Pretty *et al.*[57] who analysed the crack propagation behaviour of the material with corner crack specimens at a temperature cycle of 300 °C to 700 °C under IP, OP, CD90° and CCD90° conditions. In their study, they used a direct current potential drop (DCPD) method within an induction coil system to monitor the crack growth behaviour under transient load and thermal gradients. They found that using this approach appears to have no effect regarding potential crack tip heating or interference with the DCPD equipment and was subsequently accepted as a suitable test methodology to assess TMF crack growth rates. In terms of the results, the authors found that under the IP condition, faster crack growth rates were observed compared to OP loading, and this was attributed to the more damaging effects of high stress and temperature, leading to intergranular failure, as opposed to transgranular propagation that

was more prevalent in OP conditions. Even though Jones *et al.*[55] observed no discernible difference between the TMF lives of CD90° and CCD90° cycles in the same alloy, Pretty *et al.*[57] found there was a loading direction sensitivity present when assessing the crack growth rates, where slightly increased growth rates were seen in the CCD90° tests. They suggested that oxidation rates play a role in the change of damage mechanism between fast-moving cracks at high temperatures and those of dormant cracks, contributing to transgranular and intergranular failures in CD90° and CCD90° tests, respectively. A schematic illustration of these behaviours were previously proposed by Jones *et al.*[55], as presented in Figures 5 and 6. Varying the cycle time within tests was shown to alter the predominant crack propagation mechanism from transgranular to intergranular, highlighting the influence of time-dependent mechanisms such as oxidation.

Three subsequent publications on this topic followed in 2020 as part of the DevTMF programme.[53,59,60] Stekovic *et al.*[60] discussed the European efforts in creating a code of practice for TMF crack growth experiments, where they covered several different test-related parameters, including heating mechanisms (lamp furnace/induction), specimen types and geometries, temperature and crack growth measurement equipment, derivation of K and ΔK properties and suitable pre-cracking procedures. This exercise included a round-robin test programme, where experiments were carried out by three partnering universities, each of which employed a slightly different mechanical test approach for TMF crack growth assessments of coarse-grained RR1000. The authors found that two alternative notch geometries, namely corner crack, and single edge notch, yielded comparable TMFCG rate behaviours, resulting in consistent and comparable TMFCG rates under OP conditions that were generated at the three different laboratories. However, a differentiation in crack growth rate behaviour was observed when alternative pre-cracking approaches were employed. For instance, when pre-cracking was carried out under TMF IP test conditions, this resulted in higher TMFCG rates from tensile loading at the crack tip. However, observed crack growth variations were mitigated when compensating for crack closure. Regarding the heating methods, investigations into the impact of induction coils with various setups and radiant heating on TMF CG rates and crack tip heating did not reveal any undesired heating at the crack tip. Both heating methods studied demonstrated negligible effects on TMFCG rates. Subsequent monitoring of temperature was then discussed and whilst pyrometry and thermography were considered as favourable non-invasive techniques, they both require consistent surface emissivity during testing. Thermocouples, though less favoured for welding and complex to set up, demand rigorous control of shielding and attachment for accurate temperature measurements. Finally, the employed techniques for crack growth measurements yielded results in good agreement concerning TMFCG data. Among the 14 tested specimens, differences in CG rates were observed in only two specimens, which were attributed to the microstructural variations and crack closure.

Jones *et al.*[53] further explored the TMFCG rates of coarse grained RR1000 under different T_{Min} and T_{Max} temperatures (T_{Min} = 300 °C and 400 °C, T_{Max} = 700 °C and 750 °C) and phase angles (IP, OP, CD90° and CCD90°). In their study, they revealed a sensitivity of IP-TMFCG rates to material microstructure existed,

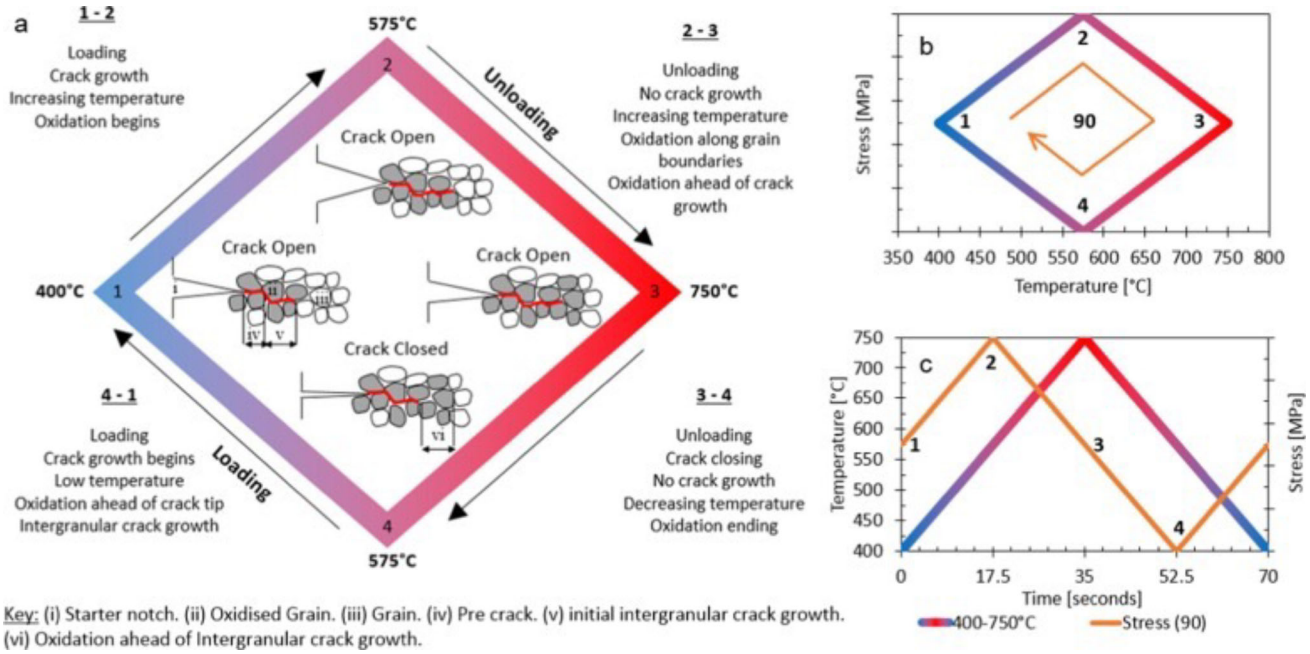

Fig. 5—(*a*) Damage mechanisms in CD (+ 90 deg) TMF cycle, 400 °C to 750 °C, (*b*) stress–temperature waveform, (*c*) applied cyclic waveforms, strain-time shown in green, temperature-time shown in red/blue (Reprinted with permission from Ref. [55]) (Color figure online).

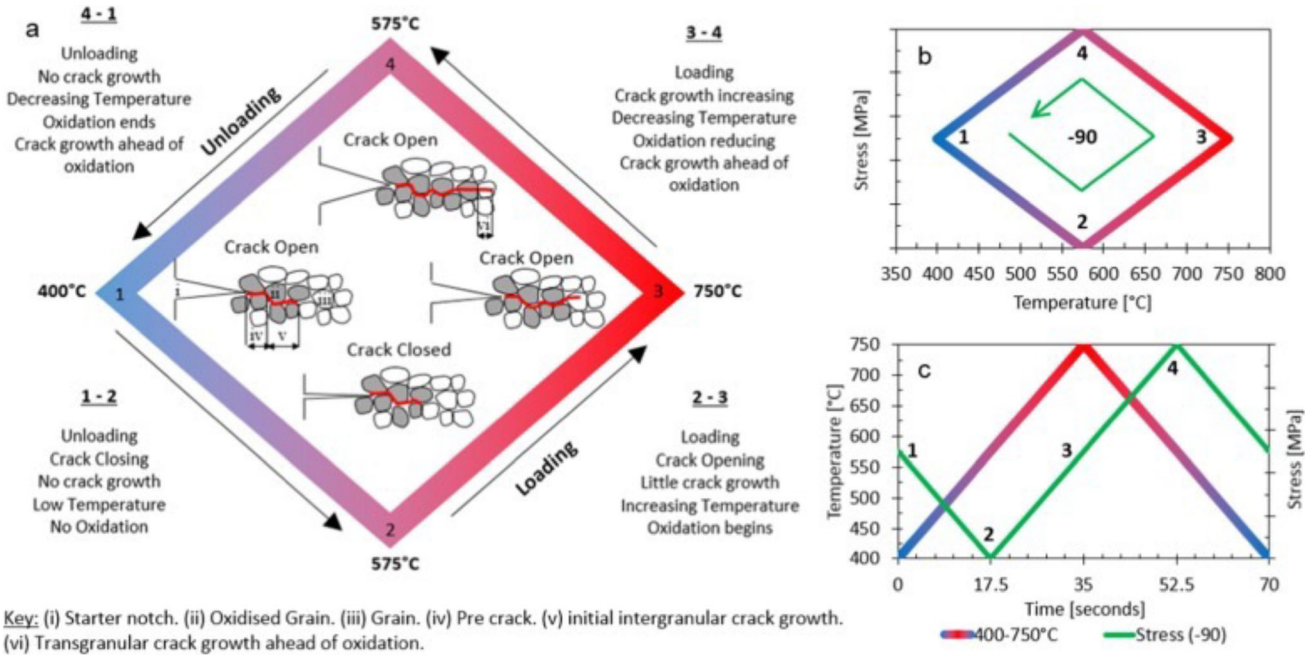

Fig. 6—(*a*) Damage mechanisms in CCD (– 90 deg) TMF cycle, 400 °C to 750 °C, (*b*) stress–temperature waveform, (*c*) applied cyclic waveforms, strain-time shown in orange, temperature-time shown in red/blue (Reprinted with permission from Ref. [55]) (Color figure online).

where a direct correlation between secondary γ' size and crack growth rate was derived. Likewise, the acceleration of IP-TMFCG rates with an increase in peak cycle temperature aligns with expectations, where faster rates were observed when T_{Max} was increased. However, a notable observation was the increase in OP crack growth rates. In the absence of evidence indicating increased oxidation formation on the fracture surface, it is proposed that stress relaxation of high compressive stresses at the crack tip accelerates crack growth when the specimen is reloaded. This effect was not observed in the fine-grained variant of the alloy, potentially due to the distinct strain-hardening behaviour of the two grain size variants. Regarding T_{Min}, no notable difference was observed when it was increased to 400 °C. The authors attributed this to the dominance of deformation mechanisms at high temperature in IP tests, while in OP tests, the crack growth rates associated with isothermal testing at 350 °C and 400 °C are not significantly different to induce a change in crack growth rates. In the tests where a diamond cycle was incorporated, different crack growth rates were evident between tests performed in a CW and CCW direction, with a lower gradient in the Paris law data for CW tests, indicating a more significant contribution of oxidation, particularly at low ΔK values.

Norman *et al.*[59] continued the efforts in this field by investigating the crack driving mechanisms in the coarse-grained variant of the material under IP and OP conditions. The variation in fatigue crack growth rates under these two loading conditions was attributed to distinct mechanical conditions at the crack tip region rather than oxidation effects. This conclusion was drawn from analyses involving digital image correlation and finite element assessments of the mechanical strain field at the crack tip. These analyses revealed that IP loading results in greater crack tip deformation and crack opening. However, quite significantly, they found that IP and OP crack growth rates align when correlated with the crack tip opening displacement. Interestingly, the IP test demonstrated a low amount of deformation in the wake of the growing crack, except for the few grains which failed transgranularly, whereas the OP test showed severe deformation around the crack area, as displayed in Figure 7. It appears that in OP crack growth, plastic deformation near the crack tip is accommodated within the grain, while grain boundary sliding is more likely in IP crack growth, owing to the increased presence of creep deformation.

4. *Summary of TMF behaviour in disc alloys*

Within this review, three main polycrystalline nickel alloys for disc applications have been evaluated in terms of TMF behaviour. IN718, Waspaloy and RR1000 represent different approaches to material design in relation to their strengthening compounds, but common themes exist in the behaviour of these alloys which can be considered here. The most extensive database of the three alloys exists on RR1000 where over the past decade extensive testing has been conducted which has encompassed the effect of phase angle, peak cycle temperature, grain size, dwell time, direction and crack propagation.

Published TMF literature is an example of data which has been heavily influenced by the practicality of experimentation associated with the testing. Published work certainly shows a preference for induction heating over infrared lamp furnaces, mainly due to cost issues, the flexibility offered by induction coils and more homogeneous heating for solid specimens. However,

whilst induction heating itself does not limit heating rates, it is recognised that excessive heating rates may give rise to undesirable thermal gradients, and hence ISO12111[1] recommends limitation of heating rates. Furthermore, cooling rates are often even more limited since either ambient or forced air cooling will likely lead to temperature differentials between the surface and centre.[61] The combination of these factors naturally leads to extended cycle times (particularly when compared to isothermal fatigue) and therefore, for practical reasons, testing programmes are generally made up of fatigue data at shorter lives, with TMF lives rarely exceeding 50,000 cycles and often restricted to less than 10,000 cycles. Work by Jones *et al.*[53][54] showed that for these shorter life tests in RR1000 a significant portion of the fatigue life is made up of crack propagation and therefore when considering these short fatigue lives, any lifing model that is proposed should consider both crack initiation and propagation phases.

The work by Pretty *et al.*[57] provided extensive information on TMF crack propagation behaviour in RR1000 with a key finding being that propagation rates could be reasonably predicted from isothermal data. Correlations were seen between TMFCG rates and isothermal data for the temperature at which the peak stress occurs within the TMF cycle. At higher temperatures, where damage mechanisms such as creep and oxidation become more prevalent, the extended cycle time within the TMF cycle for IP tests meant that rates would exceed those values from a standard trapezoidal 1–1–1–1 waveform. Yet, comparison with slower isothermal waveforms showed that these differences were predictable. Some waveforms showed subtle, yet interesting variations such as cycle direction dependency but overall, the behaviour was well understood and suitable to application in predictive lifing methods.

As stated, further work by Jones *et al.*[54] showed that for RR1000, lives shorter than 2000 cycles were dominated by crack propagation. As such it is reasonable to assume that for the IN718 data shown in Figure 8 the reduced fatigue lives shown for both 300 °C to 650 °C[46] and 350 °C to 650 °C[48] cycles can be explained again by crack propagation rates. Although the peak cycle temperature for IN718 is 50 °C lower than for RR1000, as an older alloy its overall temperature capability is also lower, and at 650 °C the alloy will be strongly influenced by time-dependent effects. IP cycles where the peak stress occurs at 650 °C will therefore show significantly faster rates than OP cycles where peak stress occurs at the T_{Min}. At temperatures such as 300 °C to 350 °C, crack propagation rates will not vary significantly and hence both 300 °C to 650 °C and 350 °C to 650 °C cycles show similar TMF lives for both IP and OP phase angles.

Waspaloy is generally regarded as a more temperature capable alloy than IN718, being employed for higher temperature operation. As such, crack propagation rates at higher temperatures in Waspaloy are reduced in comparison with IN718.[62] On this basis it is understandable that for these short TMF lives, Waspaloy outperforms IN718. A similar argument can be applied to RR1000 since the alloy was introduced to improve elevated temperature capability over Waspaloy and IN718. In the current results it can be seen that the TMF lives of RR1000 match Waspaloy, even though T_{Max} has been increased to 700 °C, indicating that RR1000 shows an improved response to elevated temperature than IN718. The data begins to become more scattered as the TMF lives increase and crack initiation life has more of an impact, but further data would be required to explore these trends.

B. *Cast Alloys for Gas Turbine Applications*

As previously discussed, the main body of TMF work in Ni-based alloys has been undertaken on single crystal alloys. This is not only due to their proximity to the hot gas stream, but also because of their low mass in

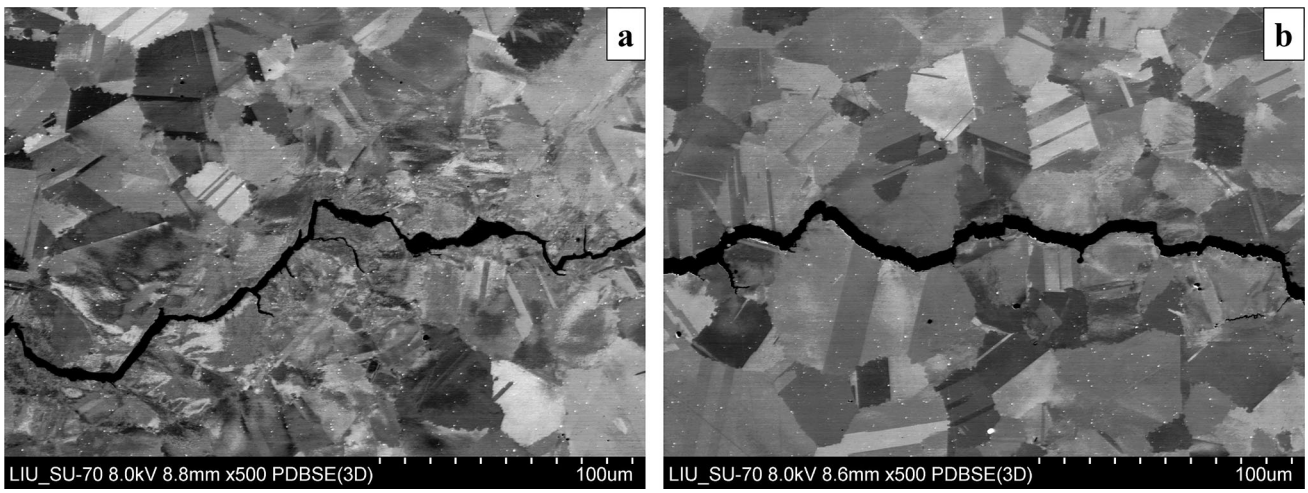

Fig. 7—Crack paths observed in RR1000 under (*a*) OP and (*b*) IP loading regimes (Reprinted from Ref. [59] under the terms of the Creative Commons CC BY license).

comparison to discs which allows for greater thermal transients and hence damage due to TMF. However, for older or downrated engines for which expensive single crystal blades are not used, a range of cast alloys have been employed for which TMF evaluation has been required. Five of these alloys are discussed here in terms of TMF behaviour: IN713, IN100, IN738LC and IN792. IN713 was one of the earliest cast alloys manufactured directly for gas turbine applications, with IN100 introduced approximately a decade later, closely followed by MarM247, IN738LC and IN792 with the specific aim of increasing blade operating temperatures. Focus would then change towards directionally solidified and single crystal alloys with the associated chemistry changes more suited to these processes.

1. *IN713LC*

Sulak *et al.*[63] investigated the impact of T_{Min} and phase shift on the TMF behaviour of Inconel 713LC (low carbon variant). TMF tests were conducted under IP and OP conditions on round bar solid specimens under a temperature regime of 300 °C to 900 °C and 500 °C to 900 °C, with a heating and cooling rate of 5 °C/s provided by an induction coil arrangement. The assessment involved analysing fatigue hardening/softening curves and the resulting fatigue life data, which concluded that the OP loading was less detrimental than the IP condition. As seen in many other Ni-based superalloys, SEM investigation showed that the life-reducing damage mechanism under IP loading was the presence of intergranular cavitation relating to creep, as shown in Figure 9. The authors also employed TEM which revealed honeycomb structures for IP loading, while plastic strain localisation into persistent slip bands was typical for OP loading, where crack growth was predominantly transgranular. The use of two different temperature regimes proved that an increase in the temperature range significantly decreased the TMF life, with a more pronounced reduction observed for OP loading. This reduction was attributed to accelerated crack propagation under high tensile stress in OP loading, along with the amount of accommodated plastic strain deformation.

Another study conducted by Sulak *et al.*[64] focused on a detailed analysis of the microstructural and mechanical behaviour of IN713LC under cyclic loading at temperatures ranging from 500 °C to 900 °C. The focus was on the effects of IP and OP loading, including a 10-minute dwell period at T_{Max}, on grain boundary stability and γ' morphology. IN713LC exhibits cyclic hardening in the OP loading while the IP loading results in mild softening due to microstructural degradation. The OP loading is less detrimental than IP at high and medium amplitudes, however, at low amplitudes, fatigue life is similar. The dominant damage mechanisms in the IP loading are attributed to creep and oxidation at grain boundaries, which lead to intergranular crack growth. At low strain amplitudes, the authors state that oxidation damage is dominant in the OP loading whereas creep damage is secondary. There is also a crossover between the IP and OP fatigue lives depending on the mechanical strain amplitudes. The 10-minute dwell leads to higher plastic strain amplitudes in cyclic stress-strain curves compared to the tests without dwell. It also significantly reduces fatigue life in both IP and OP loading. Further, the OP loading with compressive dwell forms P-type rafts, while the IP loading with tensile dwell produces N-type rafts.

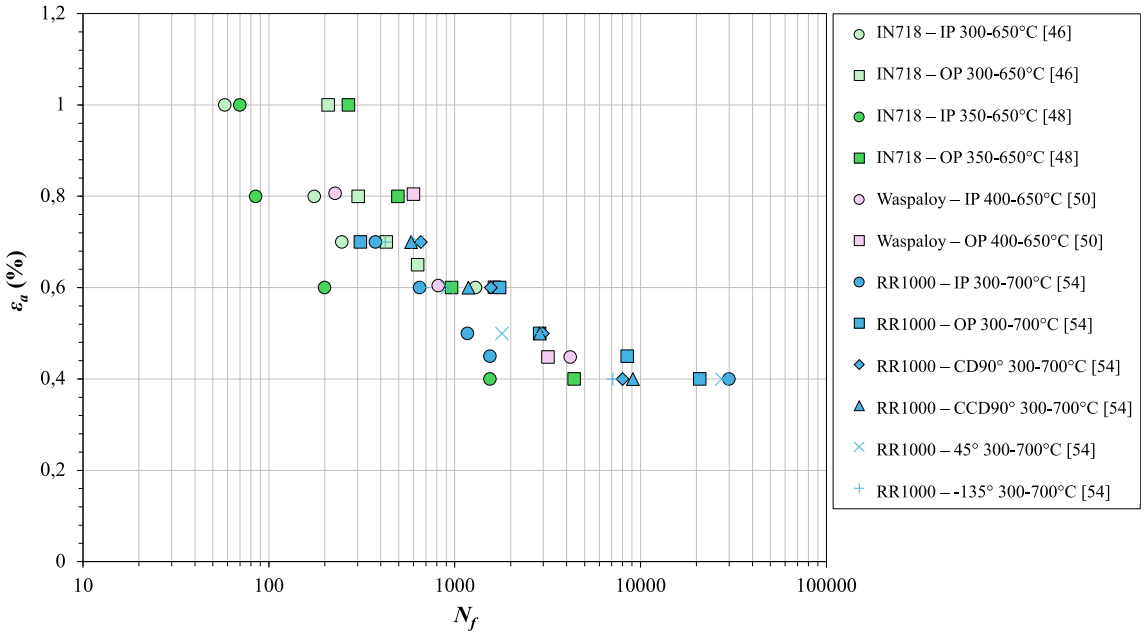

Fig. 8—Comparison of TMF behaviour in polycrystalline nickel disc alloys, IN718,[46,48] Waspaloy[50] and RR1000[54].

2. *IN100*

IN100 is a historic blade alloy which can be heat treated to optimise its trimodal distribution of precipitates. Schackert and Schweizer[65] undertook a study to understand the TMF behaviour of IN100 under two different temperature regimes, namely 300 °C to 850 °C and 300 °C to 950 °C. The authors compared the lifetimes between TMF and LCF tests at the two respective T_{Max} temperatures, and found a strong correlation existed particularly at high strain amplitudes. In general, the OP regime exhibited a longer lifetime, whilst the IP test was predominantly shorter compared to the LCF equivalents. However, this trend is not consistent at lower strain amplitudes, where the OP TMF test offered a shorter lifetime. In this case, the OP test fails at nearly 10,000 cycles, five times less than the isothermal LCF test, while the IP test reaches a runout. At an increased of T_{Max} of 950 °C, IN100 tested under TMF conditions was found to be either similar to or shorter than those of the corresponding LCF tests across two different strain levels. Yet, the OP tests consistently demonstrated higher lifetimes than the IP tests at both strain levels, since the manner of OP loading led to less cracking in the early stages of the test, whilst far greater cracks were found over the same period in the IP condition.

3. *MarM247*

MarM247 is a traditional cast nickel-base superalloy developed in the 1970s[66] which has undergone a wide range of TMF evaluation in recent years. Indeed historic papers in the field[67,68] highlight the role of MarM247 in the development of TMF understanding both in terms of experimental programmes and life prediction methodologies. In particular this early work adopted a temperature cycle of 500 °C to 871 °C to help establish behaviours which have been more widely observed as the field of TMF testing has developed. This includes crossovers in fatigue life between IP and OP TMF tests, which is usually related to the evolution of mean stress brought about by the unbalanced effects of

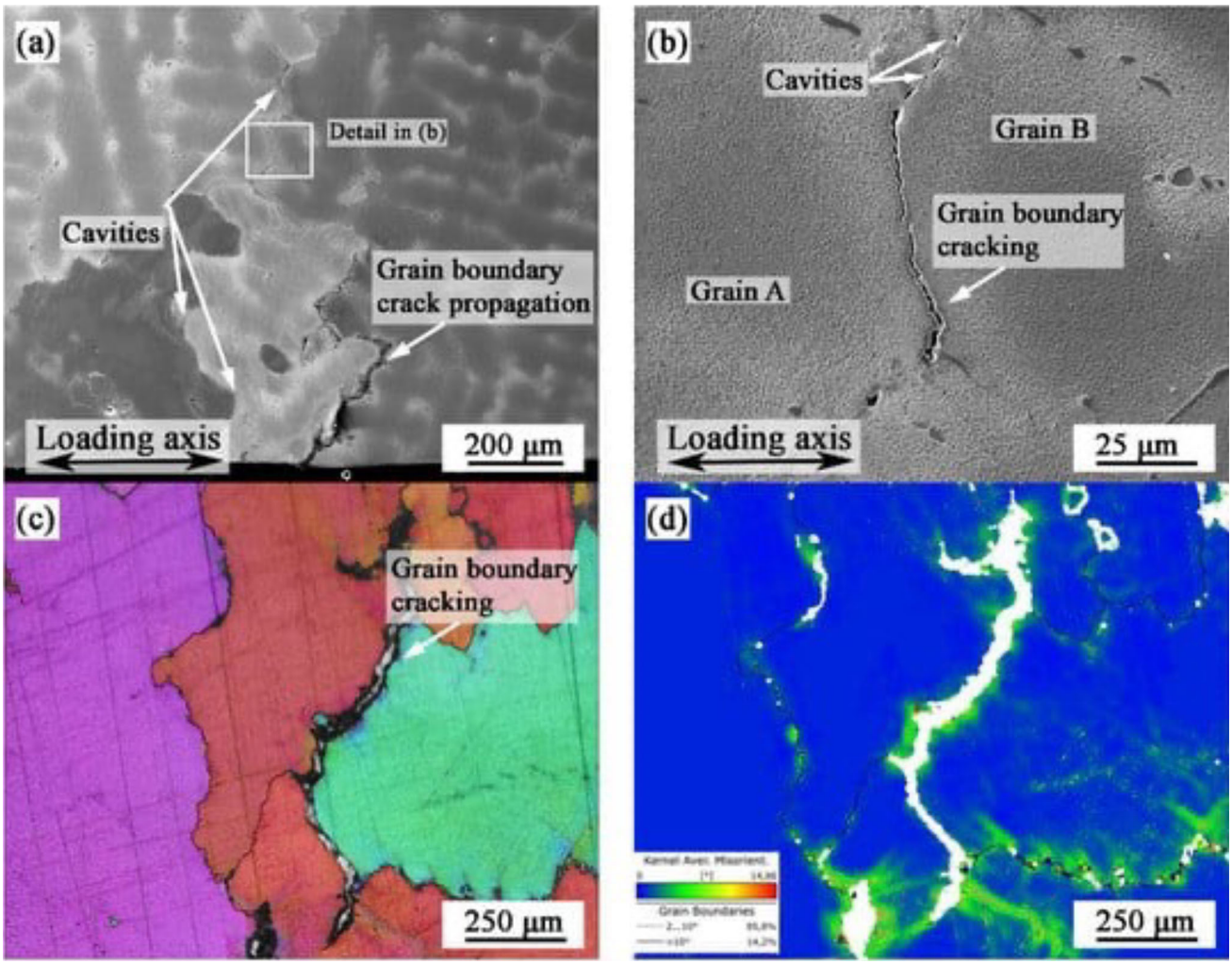

Fig. 9—TMF damage observed under IP loading (*a*) fatigue crack initiation at the grain boundary and intergranular fatigue crack propagation (*b*) detail of internal grain boundary damage (*c*) post-processed EBSD map (band contrast and inverse pole figure colouring) of internal grain boundary damage (*d*) KAM map showing local grain misorientation derived from EBSD data (Reprinted from Ref. [63] under the terms of the Creative Commons CC BY license).

high-temperature creep and lower temperature plasticity induced through deformation under TMF conditions.

More recent work, such as that performed by Sulak,[69] extended the temperature range to 500 °C to 900 °C. Interestingly this increased T_{Max} led to no crossover in the resulting fatigue curves, although a deficit in fatigue life was found under TMF loading whether under IP or OP loading when compared to isothermal fatigue. The authors conducted an in depth investigation of crack initiation and growth behaviour, finding that slip band formation was rare and found only in OP tests, and that crack growth tended to be transcrystalline for OP and mixed mode for IP tests. The work by Garcia de la Yedra *et al.*[70] on the same alloy found this to be more distinct, with intergranular fracture found in IP tests.

Alternative works by Guth *et al.*[71,72] investigated TMF cycles with a lower T_{Min} (100 °C to 850 °C) and additional phase angles in terms of diamond cycles (CD and CCD). Similar to the work by Sulak et al., the overall trend showed that IP tests exhibited the shortest fatigue lives, although this appeared to be strongly exacerbated by the lower T_{Min} and high mechanical strain amplitudes. Creep damage was found on grain boundaries in IP tests whereas high stress at low temperatures was proposed to be responsible for similar life-reducing mechanisms in OP tests.

4. *IN738LC*

In 2016, Holländer *et al.*[73] investigated the IP and OP TMF response of IN738LC at a temperature range of between 750 °C and 950 °C, with heating provided by an induction coil. In this research, they found that the TMF lives for both investigated phase conditions aligned well with the fatigue lives observed in isothermal tests conducted at 950 °C, falling within a scatter band of a factor of two. It was only at the lowest strain amplitudes that the IP and OP tests exhibited slightly longer fatigue lives compared to the comparative isothermal tests. Of the two TMF loading conditions, the IP tests offered the superior TMF performance. This behaviour was attributed to the tensile mean stresses and related higher degree of creep damage that is present under OP loading, which is not typical and occurs here only due to the high T_{Min} of the tests. However, in a similar manner to the findings reported by Kulawinski *et al.*[50], the IP and OP TMF lives could be conservatively related to the LCF lives of IN738LC at T_{Max} (950 °C).

5. *IN792*

In 2020, two experimental programmes were reported by the University of Linköping in Sweden[74,75] who studied the crack growth behaviour of IN792 under a TMF thermal cycle of 100 °C to 750 °C. Almroth *et al.*[74] compared the isothermal crack growth rate at room temperature to the behaviour seen under OP conditions on notched samples. As expected, the OP cycle was found to induce a higher crack growth rate when directly compared under the same external load, if plasticity-induced crack closure is taken into account. They found that the closure is controlled by the yield stress both in tension and compression since the crack grows under a tensile load when subjected to reversed plastic deformation. This leads to lower crack opening levels under OP conditions, indicating a higher crack driving force compared to isothermal conditions when subjected to the same T_{Min} and maximum load.

Loureiro-Homs *et al.*[75] undertook a similar investigation to compare the IP-TMF crack growth rate of IN792 compared to an isothermal equivalent at both room temperature and T_{Max}. From their results, they

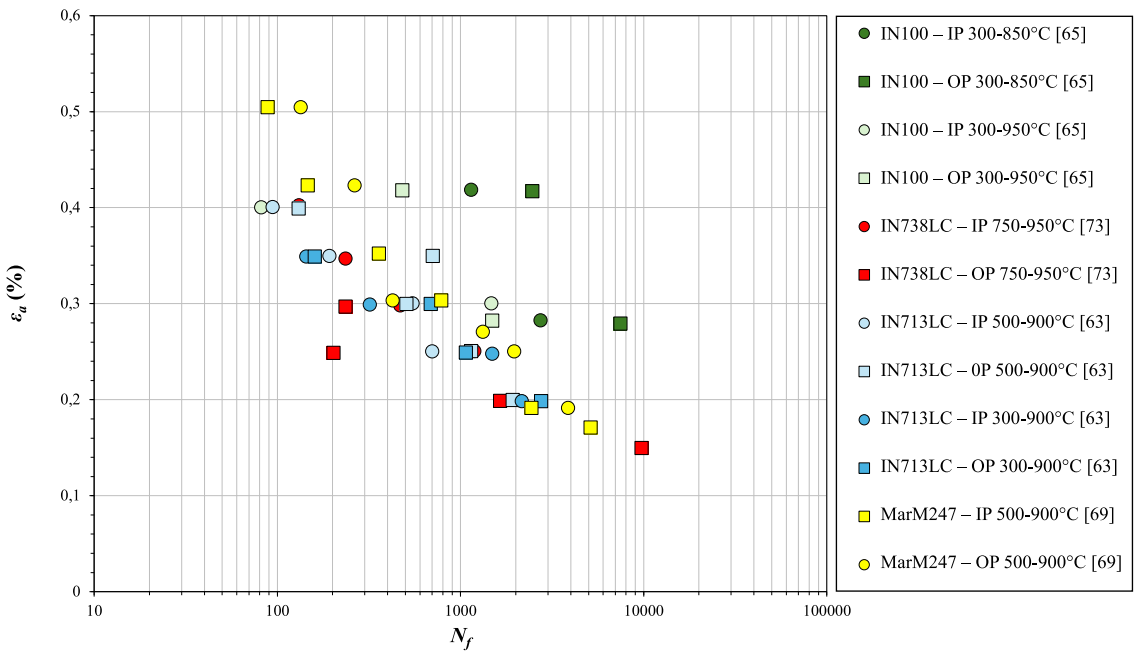

Fig. 10—Comparison of TMF behaviour in polycrystalline nickel blade alloys, IN713,[63] IN738,[73] MarM247[69] and IN100[65].

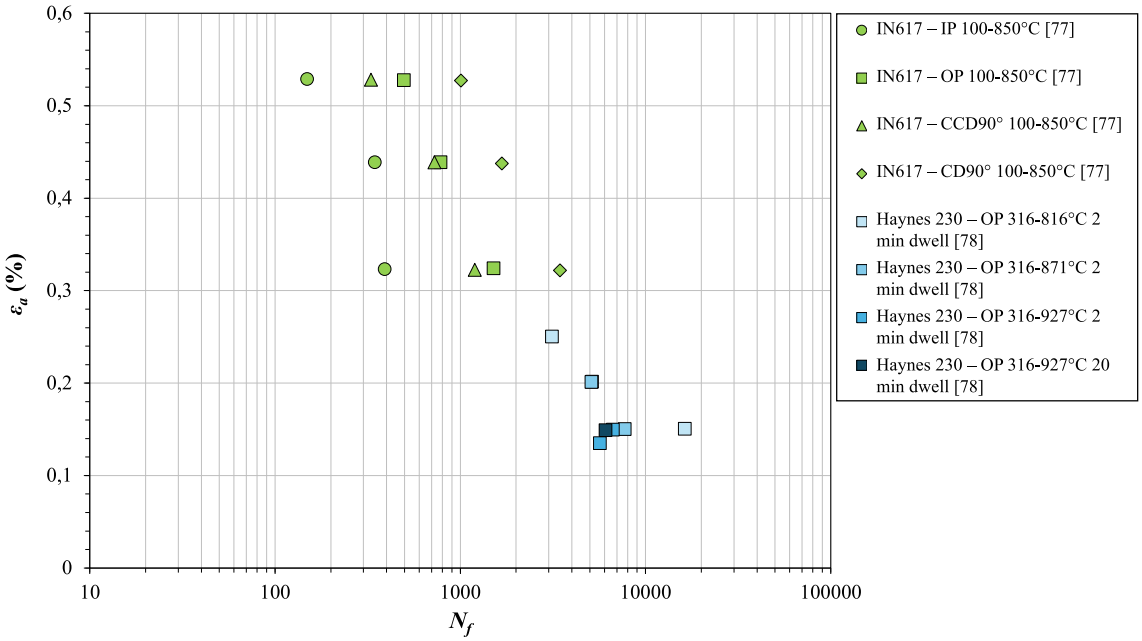

Fig. 11—Comparison of TMF behaviour in nickel combustor and other alloys, IN617[77] and Haynes 230[78].

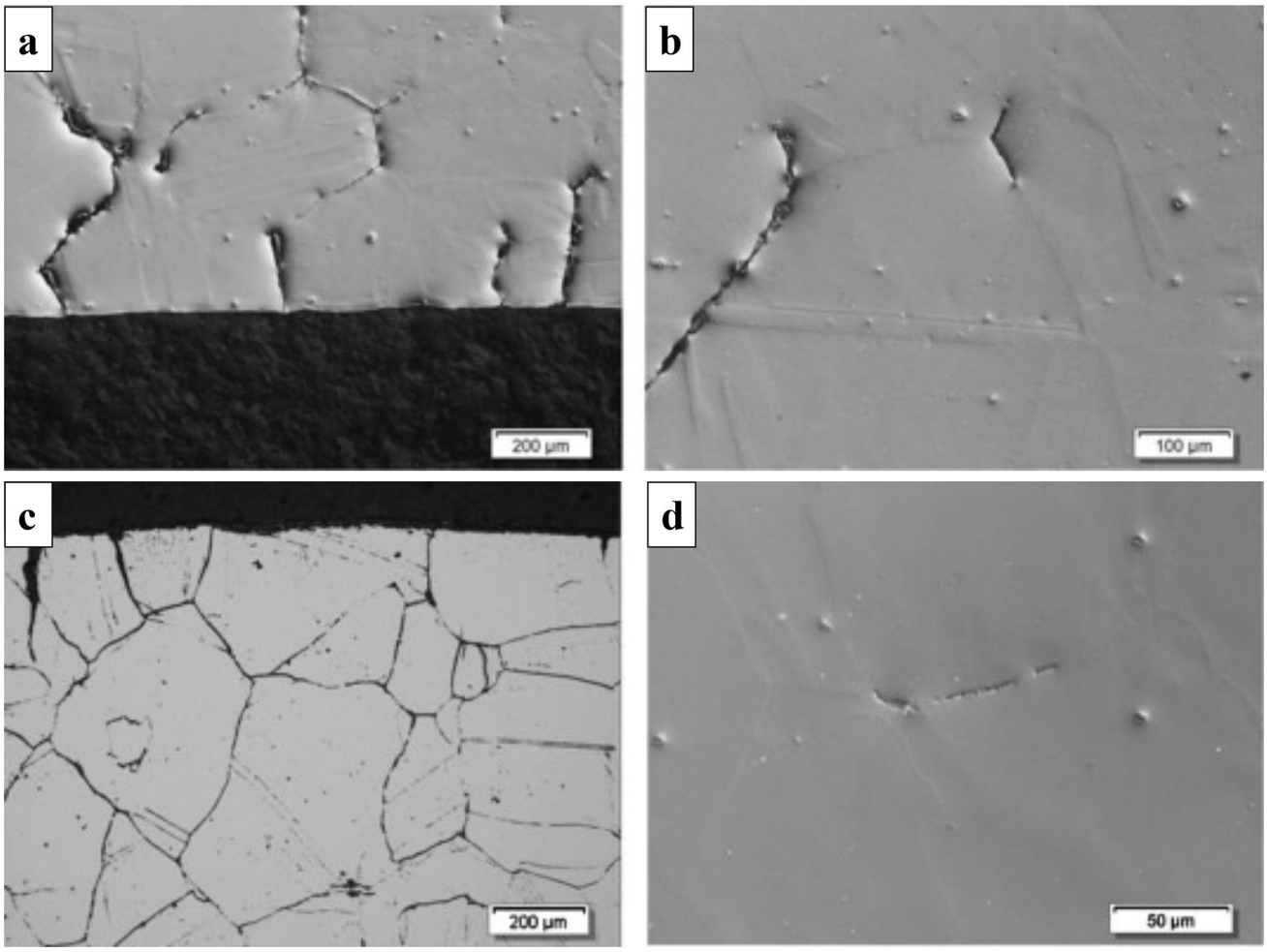

Fig. 12—Crack initiation behaviour in IN617 under IP loading, (*a*) surface, (*b*) interior; and OP loading (*c*) surface, (*d*) interior. All images were captured using differential interference contrast. The loading direction was horizontal in all images (Reprinted with permission from Ref. [77]).

revealed a significant scatter band when the crack growth rates were correlated with the linear-elastic stress intensity function, ΔK. The scatter was attributed to several possible material features, such as the microstructure, inhomogeneities in the chemical composition, and inconsistencies in the heat batches between test specimens. Previous observations suggested that the variations in residual strains generated during the initial cycles could also account for a substantial portion of the differences observed between the tests. To address this, an effective ΔK (ΔK_{eff}) was derived for each test through non-linear finite element simulations. Interestingly, when the crack propagation rates for each test were compared against the calculated ΔK_{eff}, the resulting curves converged into a narrower scatter band, providing a more cohesive representation of the data.

6. *Summary of TMF behaviour in blade alloys*

When considering blade alloys under TMF loading, as previously described, most of the published literature has considered SX-alloys, which have been the dominant alloy choice for high performance gas turbines. However, there is a small window of research where polycrystalline materials for blade alloys have received attention in terms of TMF behaviour. Figure 10 combines these results into a single graph and it is perhaps more difficult to establish trends than was the case in the disc alloys. For instance there is a clear difference between the behaviour of IN738 and IN100/IN792. In IN738, OP tests show shorter lives than IP tests, whereas the ordering is reversed for the other two alloys. In IN738 the authors attribute the reduced TMF life of the OP tests to an increased σ_{Mean}. This type of behaviour is typical of TMF tests where T_{Max} is high enough to cause significant creep deformation in the alloy and the strain range is high enough for a reasonable amount of plastic deformation. In the case where TMF life is dominated by crack initiation rather than propagation, this results in a σ_{Mean} which evolves in a tensile direction, whereas IP tests evolve in a compressive direction. This model for TMF behaviour has been previously proposed by the authors[4] and predicts a crossover in this behaviour for lower strain ranges where less plastic deformation occurs, which appears to be consistent with the behaviour of IN738 in this study.

However, in the study on IN100 the behaviour appears to be more consistent with that seen in the disc alloys described previously. The authors attribute the increased life in OP specimens to the fact that the tests are now dominated by crack propagation and that a fatigue-creep interaction occurs in IP tests which leads to a faster crack growth rate and reduction in life. Similar interpretation can be applied to the MarM247 data which also shows increased OP lives when compared to IP. The work on IN713[63] proves a little more difficult to interpret because of scatter in the data. However, the general trends appear to be similar to the IN100 and MarM247 data sets with IP tests showing shorter fatigue lives than OP in both the 300 °C to 900 °C and 500 °C to 900 °C temperature cycles. The data in this study was generated on solid cylindrical specimens and appears to point more towards a dominant crack propagation phase because of this ordering, and because the evolved σ_{Mean} values as the material deforms are not consistent with the fatigue lives as would be expected if crack initiation were dominant. Perhaps the most interesting outcome of this data however is the extended fatigue lives in the 300 °C to 900 °C tests when compared to the 500 °C to 900 °C cycle, which the authors did not provide significant detail on except to comment on the increased hardening at this temperature. Although not considered further here, it is also worth noting the research documenting the TMF behaviour of the K444 alloy, as reported by Wang *et al.*[76].

C. *Alloys for Combustor-Based Applications and Other Operations*

The static nature of gas turbine combustor casings means that behaviour is dominated by thermal stresses and resistance to high-temperature oxidation and corrosion. Wrought alloys are usually employed in a sheet form and two such alloys, IN617 and Haynes 230, are briefly discussed here along with 23Cr–45Ni–7W which has found applications for boilers and pipes. These results are presented together in Figure 11, and discussed in further detail in Sections III–C–A and III–C–B.

1. *Haynes 230*

Ahmed *et al.*[78] studied the IP and OP TMF behaviour of solid cylindrical Haynes 230 specimens under four different temperature regimes: 316 °C to 816 °C, 316 °C to 871 °C, 316 °C to 927 °C and 316 °C to 982 °C. They found that under OP conditions with a compressive dwell period, Haynes 230 experiences a σ_{Mean} evolution in the tensile direction. Conversely, in IP experiments with tensile dwells, the σ_{Mean} evolution occurs in the compressive direction. This behaviour remains consistent with previous findings[4] and appears to be the most significant parameter in determining TMF life under conditions where crack propagation does not dominate the fatigue life.

They also investigated the impact of dwells at peak strain and discovered that stress relaxation generally decreases with each cycle. Yet, in contrast, under isothermal LCF conditions with a dwell period, the total stress relaxation increases with each cycle. The authors attributed these cyclic hardening-softening responses to the T_{Max} in the TMF cycle since the fatigue lives were adversely affected by higher T_{Max} values and longer dwell periods.

2. *IN617*

Guth and Lang[77] investigated the TMF response of the Ni-based alloy NiCr22Co12Mo9, which is comparable to IN617. Various phase angles, including IP, OP, CD90° and CCD90° were employed to investigate their impact on TMF lifetime, under a temperature cycle of 100 °C to 850 °C applied *via* induction heating. The TMF lifetime exhibited a notable dependence on the phase angle, with the sequence of fatigue life ranking as IP < CCD90° < OP < CD90°. Similar to previous

work, it is difficult to reconcile the TMF lives when considering the deformation of the alloy alone. For instance, the stabilised stress range for the OP test provided in this paper far exceeds the IP tests and also shows a higher σ_{Mean}, both of which would be expected to reduce the fatigue life. However, the IP test shows a shorter life than the OP condition. It should be noted however that the fatigue lives of both IP and OP tests in the study are below 2000 cycles and therefore these results are again likely to be dominated by crack propagation, which is likely highest in IP tests when T_{Max} occurs since the crack is fully open.

Furthermore, the authors investigated the role of dwell times (2, 5, or 30 minutes) at T_{Max} under each of the four phase angles. In IP and CCD90° loading, intergranular damage predominated, whereas in OP and CD90° tests, the damage was primarily transgranular. Wedge-type cracks at grain boundary triple points were observed for all phase angles. Again, all of this information is consistent with a crack propagation dominated TMF cycle. However, the orientation of these cracks differed, being perpendicular to the loading axis for IP and CCD90° loading and parallel for OP and CD90° loading. Images of the contrasting cracking behaviours are displayed in Figure 12, for the IP and OP tests, respectively. This behaviour was attributed to phase angle-dependent grain boundary sliding. The introduction of dwell times resulted in lower stress amplitudes and higher plastic strain amplitudes compared to tests without dwells. Interestingly, for OP and CD90° loading, these two effects appeared to offset each other, yielding a minor overall impact on lifetime. Yet in contrast, for IP and CCD90° loading, the reduction in intergranular damage due to lower tensile stress at high temperatures resulted in an increased TMF life when dwells were introduced.[69]

3. *23Cr–45Ni–7W*

Noguchi *et al.*[79] conducted a series of TMF experiments on a Ni-based superalloy consisting of 23Cr–45Ni–7W. They employed a temperature range of 100 °C to 700 °C and studied the IP and OP response of the material. The authors found that under the same total strain range, the lives under IP conditions were 0.30 to 0.44 times shorter than that of the OP conditions. This difference was attributed to the nature of crack growth, where intergranular cracking occurred under a cyclic tensile creep strain seen in the IP regime, while transgranular cracking prevailed under cyclic compressive creep strain during the OP tests. Again, the findings of these authors are consistent with previous TMF data presented earlier in this article, with short fatigue lives in that crack propagation dominates and IP lives tend to be the shortest.

4. *Summary of TMF behaviour in combustor alloys*

Whilst combustor alloys have not undergone extensive evaluation under TMF loading, it is encouraging to note that the basic trends in the data appear comparable with blade and disc alloys. In particular, one of the main drivers appears to be the peak cycle temperature, since high temperatures allow for creep deformation which promotes mean stress evolution. Mean stress can then often be related to overall TMF life. Dwell effects only further promote this mean stress shift and will often exaggerate effects. A second driver that should be noted however is that the ordering of phase angle data may be dependent on the overall life with shorter tests being dominated by crack propagation which is generally faster in IP tests and hence show shorter fatigue lives.

IV. CONCLUSIONS

It is clear that for an experimentally challenging mechanical test such as TMF, development of test facilities has played a big role in the generation of reliable test data from which more detailed understanding of material behaviour can be derived. However, since the development of ISO12111, ASTM2368 and ISO23296:2022, the field has continued to further develop as shown by much of the research detailed in this review. Clear trends within the published data for SX-alloys can be summarised as:

- Damage mechanisms during TMF in SX-alloys include fatigue, creep, and oxidation, with microstructural degradation such as γ' precipitate coarsening, rafting, recrystallisation, and TCP-phase formation playing crucial roles.
- In IP-TMF cycles, tensile loading at high temperatures and compressive loading at low temperatures promote creep in tension and plasticity in compression.
- OP TMF cycles involve creep relaxation in compression at high temperatures and plastic deformation in tension at low temperatures, typical in "hot-spot" areas of turbine blades. The formation of brittle oxides at high temperatures further reduces OP–TMF life by promoting cracking during tension at lower temperatures.
- The formation of the deformation bands is critical to TMF damage in SX-alloys, and is dependent on factors such as crystal orientation, phase angle, and dwell time.
- In a strain-controlled TMF test of SX-alloys, the elastic stiffness in the loading direction significantly influences TMF life for a given mechanical strain range. A higher number of active slip systems during deformation is beneficial in OP TMF as it leads to more widespread and less localised deformation.
- Creep was identified as the predominant damage mechanism in IP-TMF, while oxidation contributed to shorter life in OP TMF tests.

Since CMSX-4 has become the industry standard for single crystal turbine blades operating at high temperatures it is not surprising that the published research is perhaps more in depth for this particular alloy and shows more mechanistic understanding. However, in the field of polycrystalline alloys, increased data quality now allows for the development of lifing approaches which can be applied more generically across alloy variants,

leading to an improved understanding within the field, as demonstrated within this paper. The main findings of the review have concluded:

- TMF testing of polycrystalline alloys allows for alternative heating methods to induction coils to be used, such as lamp furnaces. However, the heating type can have an effect on the homogeneity of temperature within tests and should be considered, along with cycle time, to reduce potentially detrimental thermal gradients.
- Since disc alloys are often lifed using a damage tolerance methodology, it is important to understand the relative contributions of crack initiation and propagation to total fatigue life, and in particular the TMF crack propagation rates which occur.
- Higher quality data in recent years has implied that TMF data can usually be well understood based on the relative contributions of fatigue, creep and oxidation which may be influenced by the applied phase angle. Provided these contributions are well understood, meaningful correlations with isothermal data are possible.

FUNDING

Open access funding provided by Linköping University.

CONFLICT OF INTEREST

On behalf of all authors, the corresponding author states that there is no conflict of interest.

OPEN ACCESS

REFERENCES

1. ISO: *ISO 12111:2011: Metallic Materials: Fatigue Testing: Strain-Controlled Thermomechanical Fatigue Testing Method*, ISO, 2011.
2. ASTM International: *ASTM Standard E 2368-04, Standard Practice for Strain Controlled Thermomechanical Fatigue Testing*, ASTM International, 2004.
3. ISO: *ISO23296:2022 Metallic Materials – Fatigue Testing – Force Controlled Thermo-Mechanical Fatigue Testing method*, ISO, 2022.
4. R.J. Lancaster, M.T. Whittaker, and S.J. Williams: *Mater. High Temp.*, 2013, vol. 30(1), pp. 2–12. https://doi.org/10.3184/096034013X13630238172260.
5. P. Zhang, Q. Zhu, G. Chen, and C. Wang: *Mater. Trans.*, 2015, vol. 56(12), pp. 1930–39. https://doi.org/10.2320/matertrans.M2015323.
6. R.C. Reed: *The Superalloys: Fundamentals and Applications*, Cambridge University Press, Cambridge, 2008.
7. J.J. Moverare, S. Johansson, and R.C. Reed: *Acta Mater.*, 2009, vol. 57(7), pp. 2266–76. https://doi.org/10.1016/j.actamat.2009.01.027.
8. K. Harris and J.B. Wahl: in *Superalloys 2004 (Tenth International Symposium)*, TMS, 2004, pp. 45–52. https://doi.org/10.7449/2004/Superalloys_2004_45_52.
9. J. Xu and H. Yuan: *Eng. Fract. Mech.*, 2024, vol. 297, 109871https://doi.org/10.1016/j.engfracmech.2024.109871.
10. J.J. Moverare and R.C. Reed: *MATEC Web of Conferences*, vol. 14, 2014, p. 06001. https://doi.org/10.1051/matecconf/20141406001.
11. M. Segersäll, D. Leidermark, and J.J. Moverare: *Mater. Sci. Eng. A*, 2015, vol. 623, pp. 68–77. https://doi.org/10.1016/j.msea.2014.11.026.
12. R.W. Neu: *Int. J. Fatigue*, 2019, vol. 123, pp. 268–78. https://doi.org/10.1016/j.ijfatigue.2019.02.022.
13. M. Segersäll and D. Deng: *Int. J. Fatigue*, 2021, vol. 146, 106162https://doi.org/10.1016/j.ijfatigue.2021.106162.
14. C. Luo and H. Yuan: *Int. J. Fatigue*, 2023, vol. 168, 107438https://doi.org/10.1016/j.ijfatigue.2022.107438.
15. R. Smith, R. Lancaster, J. Jones, and J. Mason-Flucke: *Materials*, 2019, vol. 12(6), p. 998. https://doi.org/10.3390/ma12060998.
16. R.L. Amaro, S.D. Antolovich, and R.W. Neu: *Fatigue Fract. Eng. Mater. Struct.*, 2012, vol. 35(7), pp. 658–71. https://doi.org/10.1111/j.1460-2695.2011.01660.x.
17. G.M. Han, J.J. Yu, X.F. Sun, and Z.Q. Hu: *Mater. Sci. Eng. A*, 2011, vol. 528(19–20), pp. 6217–24. https://doi.org/10.1016/j.msea.2011.04.083.
18. H.U. Hong, J.G. Kang, B.G. Choi, I.S. Kim, Y.S. Yoo, and C.Y. Jo: *Int. J. Fatigue*, 2011, vol. 33(12), pp. 1592–99. https://doi.org/10.1016/j.ijfatigue.2011.07.009.
19. R.K. Kersey, A. Staroselsky, D.C. Dudzinski, and M. Genest: *Int. J. Fatigue*, 2013, vol. 55, pp. 183–93. https://doi.org/10.1016/j.ijfatigue.2013.06.006.
20. F. Palmert, J. Moverare, and D. Gustafsson: *Int. J. Fatigue*, 2019, vol. 122, pp. 184–98. https://doi.org/10.1016/j.ijfatigue.2019.01.014.
21. J. Yang, F. Jing, Z. Yang, K. Jiang, D. Hu, and B. Zhang: *J. Alloys Compd.*, 2021, vol. 872, 159578https://doi.org/10.1016/j.jallcom.2021.159578.
22. X. Ai, L. Shi, F. Luo, H. Pei, and Z. Wen: *Eng. Fract. Mech.*, 2023, vol. 284, 109262https://doi.org/10.1016/j.engfracmech.2023.109262.
23. J.J. Moverare, M. Segersäll, A. Sato, S. Johansson, and R.C. Reed: *Superalloys 2012*, Wiley, 2012, pp. 369–77. https://doi.org/10.1002/9781118516430.ch40.
24. F. Sun, J. Zhang, and H. Harada: *Acta Mater.*, 2014, vol. 67, pp. 45–57. https://doi.org/10.1016/j.actamat.2013.12.011.
25. M. Segersäll, J.J. Moverare, K. Simonsson, and S. Johansson: in *Superalloys 2012*, Wiley, 2012, pp. 215–23. https://doi.org/10.1002/9781118516430.ch24.
26. J.X. Zhang, H. Harada, Y. Koizumi, and T. Kobayashi: *Scr. Mater.*, 2009, vol. 61(12), pp. 1105–08. https://doi.org/10.1016/j.scriptamat.2009.08.036.
27. R. Wang, B. Zhang, D. Hu, K. Jiang, X. Hao, J. Mao, and F. Jing: *Int. J. Fatigue*, 2019, vol. 126, pp. 327–34. https://doi.org/10.1016/j.ijfatigue.2019.05.016.
28. F. Palmert, P. Almroth, D. Gustafsson, J. Loureiro-Homs, A. Saxena, and J. Moverare: *Int. J. Fatigue*, 2021, vol. 144, 106074https://doi.org/10.1016/j.ijfatigue.2020.106074.
29. F. Mauget, F. Hamon, M. Morisset, J. Cormier, F. Riallant, and J. Mendez: *Int. J. Fatigue*, 2017, vol. 99, pp. 225–34. https://doi.org/10.1016/j.ijfatigue.2016.08.001.
30. S.S. Ezz, D.P. Pope, and V. Paidar: *Acta Metall.*, 1982, vol. 30(5), pp. 921–26. https://doi.org/10.1016/0001-6160(82)90198-5.

31. D. Arrell, M. Hasselqvist, C. Sommer, and J. Moverare: in *Proceedings of the International Symposium on Superalloys*, eds, K.A. Green, T.M. Pollock, H. Harada, T.E. Howson, R.C. Reed, J.J. Schirra, and S. Walston, The Minerals, Metals and Materials Society, TMS, Warrendale, 2004, pp. 291–94.
32. R.A. Kupkovits, D.J. Smith, and R.W. Neu: *Procedia Eng*, 2010, vol. 2(1), pp. 687–96. https://doi.org/10.1016/j.proeng.2010.03.074.
33. D. Leidermark, J.J. Moverare, S. Johansson, K. Simonsson, and S. Sjöström: *Acta Mater.*, 2010, vol. 58(15), pp. 4986–97. https://doi.org/10.1016/j.actamat.2010.05.032.
34. M.M. Kirka, K.A. Brindley, R.W. Neu, S.D. Antolovich, S.R. Shinde, and P.W. Gravett: *Int. J. Fatigue*, 2015, vol. 81, pp. 191–201. https://doi.org/10.1016/j.ijfatigue.2015.08.001.
35. F. Sun, S. Zhang, S. Tian, J. Zhang, and H. Harada: *Mater. Sci. Technol.*, 2015, vol. 31(2), pp. 237–42. https://doi.org/10.1179/1743284714Y.0000000520.
36. B. Fu, J. Zhang, and H. Harada: *Prog. Nat. Sci. Mater. Int.*, 2013, vol. 23(5), pp. 508–513. https://doi.org/10.1016/j.pnsc.2013.09.005.
37. B.D. Fu, J.X. Zhang, and H. Harada: *Mater. Sci. Eng. A*, 2014, vol. 605, pp. 253–59. https://doi.org/10.1016/j.msea.2014.03.060.
38. X.Z. Lv, J.X. Zhang, and H. Harada: *J. Mater. Eng. Perform.*, 2014, vol. 23(3), pp. 766–71. https://doi.org/10.1007/s11665-013-0809-3.
39. X.Z. Lv, J.X. Zhang, and H. Harada: *Int. J. Fatigue*, 2014, vol. 66, pp. 246–51. https://doi.org/10.1016/j.ijfatigue.2014.04.012.
40. M. Kolbe: *Mater. Sci. Eng. A*, 2001, vol. 319–321, pp. 383–87. https://doi.org/10.1016/S0921-5093(01)00944-3.
41. M. Segersäll, J.J. Moverare, K. Simonsson, and S.L Johansson: in *Superalloys 2012*, Wiley, 2012, pp. 215–23. https://doi.org/10.1002/9781118516430.ch24.
42. J.J. Moverare and S. Johansson: *Mater. Sci. Eng. A*, 2010, vol. 527(3), pp. 553–58. https://doi.org/10.1016/j.msea.2009.08.023.
43. A. Sato, J.J. Moverare, M. Hasselqvist, and R.C. Reed: *Metall. Mater. Trans. A.*, 2012, vol. 43A(7), pp. 2302–2315. https://doi.org/10.1007/s11661-011-0995-2.
44. M. Segersäll, P. Kontis, S. Pedrazzini, P.A.J. Bagot, M.P. Moody, J.J. Moverare, and R.C. Reed: *Acta Mater.*, 2015, vol. 95, pp. 456–67. https://doi.org/10.1016/j.actamat.2015.03.060.
45. Z. Ge, G. Xie, M. Segersäll, V. Norman, Z. Chen, J. Moverare, L. Lou, and J. Zhang: *Int. J. Fatigue*, 2022, vol. 156, 106634https://doi.org/10.1016/j.ijfatigue.2021.106634.
46. J. Sun and H. Yuan: *Int. J. Fatigue*, 2019, vol. 119, pp. 89–101. https://doi.org/10.1016/j.ijfatigue.2018.09.017.
47. J. Sun, H. Yuan, and M. Vormwald: *Int. J. Fatigue*, 2020, vol. 135, 105486https://doi.org/10.1016/j.ijfatigue.2020.105486.
48. W. Deng, J. Xu, Y. Hu, Z. Huang, and L. Jiang: *Mater. Sci. Eng. A*, 2019, vol. 742, pp. 813–19. https://doi.org/10.1016/j.msea.2018.11.052.
49. M. Böcker, H.R. Babu, S. Henkel, M. Raddatz, U. Gampe, and H. Biermann: *Metall. Mater. Trans. A.*, 2023, vol. 54A(5), pp. 1971–84. https://doi.org/10.1007/s11661-022-06885-x.
50. D. Kulawinski, A. Weidner, S. Henkel, and H. Biermann: *Int. J. Fatigue*, 2015, vol. 81, pp. 21–36. https://doi.org/10.1016/j.ijfatigue.2015.07.020.
51. M. Clavel and A. Pineau: *Scr. Metall.*, 1982, vol. 16(4), pp. 361–64. https://doi.org/10.1016/0036-9748(82)90150-8.
52. M. Clavel and A. Pineau: *Mater. Sci. Eng.*, 1982, vol. 55(2), pp. 157–71. https://doi.org/10.1016/0025-5416(82)90129-X.
53. J. Jones: in *Encyclopedia of Materials: Metals and Alloys*, Elsevier, 2022, pp. 476–84. https://doi.org/10.1016/B978-0-12-819726-4.00112-5.
54. J. Jones, M. Whittaker, R. Lancaster, and S. Williams: *Int. J. Fatigue*, 2017, vol. 98, pp. 279–85. https://doi.org/10.1016/j.ijfatigue.2017.01.036.
55. J. Jones, M. Whittaker, R. Lancaster, C. Hyde, J. Rouse, B. Engel, S. Pattison, S. Stekovic, C. Jackson, and H.Y. Li: *Int. J. Fatigue*, 2020, vol. 135, 105539https://doi.org/10.1016/j.ijfatigue.2020.105539.
56. V. Gray, J.P. Jones, M.T. Whittaker, R.J. Lancaster, C.J. Pretty, and S.J. Williams: *Int. J. Fatigue*, 2022, vol. 156, 106631https://doi.org/10.1016/j.ijfatigue.2021.106631.
57. C. Pretty, M. Whitaker, and S. Williams: *Materials*, 2017, vol. 10(1), p. 34. https://doi.org/10.3390/ma10010034.
58. M. Whittaker, R. Lancaster, W. Harrison, C. Pretty, and S. Williams: *Materials*, 2013, vol. 6(11), pp. 5275–90. https://doi.org/10.3390/ma6115275.
59. V. Norman, S. Stekovic, J. Jones, M. Whittaker, and B. Grant: *Int. J. Fatigue*, 2020, vol. 135, 105528https://doi.org/10.1016/j.ijfatigue.2020.105528.
60. S. Stekovic, J.P. Jones, B. Engel, M.T. Whittaker, V. Norman, J.P. Rouse, S. Pattison, C.J. Hyde, P. Härnman, R.J. Lancaster, D. Leidermark, and J. Moverare: *Int. J. Fatigue*, 2020, vol. 138, 105675https://doi.org/10.1016/j.ijfatigue.2020.105675.
61. J. Palmer, J. Jones, M. Whittaker, and S. Williams: *Materials*, 2022, vol. 15(18), p. 6264. https://doi.org/10.3390/ma15186264.
62. X. Liu, S. Rangararan, E. Barbero, K.-M. Chang, W. Cao, R. Kennedy, and T. Carneiro: in *Superalloys 2004 (10th International Symposium)*, TMS, 2004.
63. I. Šulák, K. Hrbáček, and K. Obrtlík: *Metals*, 2022, vol. 12(6), p. 993. https://doi.org/10.3390/met12060993.
64. I. Šulák and K. Obrtlík: *Int. J. Fatigue*, 2023, vol. 166, 107238https://doi.org/10.1016/j.ijfatigue.2022.107238.
65. S.M. Schackert and C. Schweizer: *Fatigue Fract. Eng. Mater. Struct.*, 2022, vol. 45(8), pp. 2261–76. https://doi.org/10.1111/ffe.13733.
66. K. Harris, G.L. Erickson, and R.E. Schwer: in *Superalloys 1984 (5th International Symposium)*, TMS, 1984, pp. 221–30. https://doi.org/10.7449/1984/Superalloys_1984_221_230.
67. D.A. Boismier and H. Sehitoglu: *J. Eng. Mater. Technol.*, 1990, vol. 112(1), pp. 68–79. https://doi.org/10.1115/1.2903189.
68. H. Sehitoglu and D.A. Boismier: *J. Eng. Mater. Technol.*, 1990, vol. 112(1), pp. 80–89. https://doi.org/10.1115/1.2903191.
69. I. Šulák and K. Obrtlík: *Theoret. Appl. Fract. Mech.*, 2024, vol. 131, 104443https://doi.org/10.1016/j.tafmec.2024.104443.
70. A. García de la Yedra, J.L. Pedrejón, and A. Martín-Meizoso: *Mater. High Temp.*, 2013, vol. 30(1), pp. 19–26. https://doi.org/10.3184/096034013X13631630183856.
71. S. Guth, S. Doll, and K.-H. Lang: *Mater. Sci. Eng. A*, 2015, vol. 642, pp. 42–48. https://doi.org/10.1016/j.msea.2015.06.055.
72. S. Guth, S. Doll, and K.-H. Lang: *Procedia Eng*, 2014, vol. 74, pp. 269–72. https://doi.org/10.1016/j.proeng.2014.06.260.
73. D. Holländer, D. Kulawinski, M. Thiele, C. Damm, S. Henkel, H. Biermann, and U. Gampe: *Mater. Sci. Eng. A*, 2016, vol. 670, pp. 314–24. https://doi.org/10.1016/j.msea.2016.05.114.
74. P. Almroth, D. Gustafsson, J. Loureiro Homs, and K. Simonsson: *Int. J. Fatigue*, 2020, vol. 141, 105906https://doi.org/10.1016/j.ijfatigue.2020.105906.
75. J. Loureiro-Homs, D. Gustafsson, P. Almroth, K. Simonsson, R. Eriksson, and D. Leidermark: *Int. J. Fatigue*, 2020, vol. 136, 105569https://doi.org/10.1016/j.ijfatigue.2020.105569.
76. R. Wang, B. Zhang, D. Hu, K. Jiang, H. Liu, J. Mao, F. Jing, and X. Hao: *Eng. Fail. Anal.*, 2019, vol. 102, pp. 35–45. https://doi.org/10.1016/j.engfailanal.2019.04.023.
77. S. Guth and K.-H. Lang: *Int. J. Fatigue*, 2017, vol. 99, pp. 286–94. https://doi.org/10.1016/j.ijfatigue.2016.10.015.
78. R. Ahmed, P.R. Barrett, M. Menon, and T. Hassan: *Int. J. Solids Struct.*, 2017, vol. 126–127, pp. 90–104. https://doi.org/10.1016/j.ijsolstr.2017.07.033.
79. Y. Noguchi, H. Okada, H. Semba, M. Yoshizawa, and F. Minami: *Int. J. Fatigue*, 2018, vol. 112, pp. 253–62. https://doi.org/10.1016/j.ijfatigue.2018.03.026.